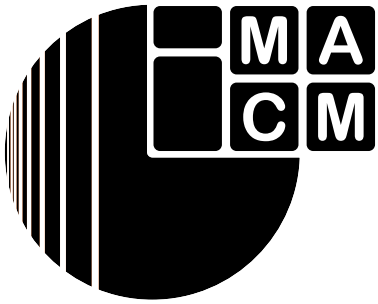

Bergische Universität Wuppertal

Fachbereich Mathematik und Naturwissenschaften

Institute of Mathematical Modelling, Analysis and Computational Mathematics
(IMACM)

Preprint BUW-IMACM 13/34

Andreas Bartel and Michael Günther

PDAEs in Refined Electrical Network Modelling

December 11, 2013

http://www.math.uni-wuppertal.de

PDAEs in Refined Electrical Network Modelling

Andreas Bartel and Michael Günther

Abstract Modelling with partial differential-algebraic equations (PDAEs) is a natural and universal approach valid for various applications with coupled subsystems. This contribution summarizes the state of PDAEs as models in the simulation of electric circuits. We mainly discusses the modelling and analysis aspects of several important settings. In the modelling we embed the network equations into the context of Maxwell's equations and address the main three types of coupling: modelling with subsystems of the same type, refined models and multiphysics. In the analysis part we address the aspect of the existence of solutions for these complex systems as well as structural properties as the DAE index (after spatial semi-discretization). For the numerical simulation, we give results for the cosimulation technique (also referred to as dynamic iteration), which is a standard method for coupled systems.

1 Introduction

In electric circuit design, a mathematical model is deduced from a network approach [31]. It yields time-dependent systems of differential algebraic equations (DAEs) with voltages and currents as state variables. This network approach is a very powerful tool, which is used in many other applications, too. It is also employed to describe, for example, multibody systems with plasticity [18], in multibody systems in mechanics and vehicle system dynamics [16], river flow models in computational fluid dynamics [43], blood circulation in life sciences [45] or gas networks [23].

In the world of electrical systems, a lumped network description is obtained based on two types of information: (1) branch relations, which describe various electric effects: voltage source, current source, resistance, capacitance, inductance (so-called basic elements); and (2) pure topological information, which describe the ideal shunt of the branches. On the one hand, usually the exact spatial

Andreas Bartel
Bergische Universität Wuppertal, Applied Mathematics and Numerical Analysis, 42097 Wuppertal, Germany, e-mail: bartel@math.uni-wuppertal.de

Michael Günther
Bergische Universität Wuppertal, Applied Mathematics and Numerical Analysis, 42097 Wuppertal, Germany, e-mail: guenther@math.uni-wuppertal.de

location and distributive nature of these elements can be disregarded. Hence they are considered as ideally shunt lumped elements and the topology information is represented by incidence matrices alone. On the other hand, the branch relations specify the physical behaviour of the basic elements (branches). Basically this is realized via current-voltage relations.

However, downscaling in electric circuit design brought us to nanoscales. In consequence, formerly disregarded secondary effects require now more detailed models. Such effects are due to the distributive nature of elements or due to impact of other physical quantities, for instance. Hence *refined* or *multiphysically extended models* are necessary. These define coupled systems of DAEs and PDEs and are abbreviated as PDAEs:

a) refined models: the simple basic, 0D electric network element is replaced by a more complex PDE model, where in the end, a current-voltage relation is described. To state the coupling, we have the node voltages of the network together with the device currents. The coupling conditions are given as boundary conditions of the PDE system and they link DAE and PDE quantities. From the perspective of standard electric network modelling, the evaluation of the basic model is replaced by the evaluation of a more complex model, where the circuit simulator has to be linked to the solution of a PDE system.
b) multiphysically extended models: here a new physical domain is added to the electric circuit variables to describe the impact of other physical quantities on the electric network. Generally in this case, the coupling is much more complex and specialized. The coupling is realized via source terms and via parameter dependences, where for instance a network parameter becomes a possibly nonlinear function of the PDE quantities.

This paper deals with modelling, analysing and numerically solving such coupled PDAE systems stemming from both refined and multiphysically extended models in electric circuit simulation. There will be no homogeneous theory of such system due to the wide range of possible model constructions. However, as we will see, these models share structural similarities, which can be exploited during analysis and numerical simulation.

This paper is organized as follows: in Section 2 electric network models, derived from Maxwell's equations, are introduced. We discuss the DAE aspects of this modelling concept. The following Section 3 discusses different ways of deriving coupled systems based on electrical network models in its core: a) network-network coupling, defining coupled DAE-DAE systems, when subcircuits or companion models are linked to each other; b) refined PDAE modelling, if a network element is replaced by a refined PDE description, for example, semiconductor devices, transmission lines and inductive elements; c) multiphysics coupling, if the network is linked to a PDE system describing a further physical domain such as thermal effects. The analytical properties of the coupled systems introduced in Section 3 are discussed in Section 4. Here we concentrate on index analysis and existence/uniqueness results. With co-simulation, a tailored approach is discussed in Section 5 to efficiently solve coupled systems introduced and analysed in the previous sections. We finish with a short conclusion in Section 6.

2 Modelling of Electric Networks

The simulation of real electrical circuits is based on a network approach, where circuits are described by an ideal shunt of subsystems or basic elements. Thus a network model consists of a description

of the interconnects (network graph), electro(-magnetic) model for the subsystems and Kirchhoff's laws for the ideal interconnection — see e.g. [31, 44] for a detailed introduction. Such a lumped model is derived from Maxwell's equations. This will be also our starting point. First we recall Maxwell's equations. Then we derive the network model from Maxwell's equations, which is a differential-algebraic equation (DAE). Subsequently we state important DAE properties of this model. Finally, we point out the general character of the network approach, which applies also to other applications.

2.1 Maxwell's Equations

The classical Maxwell's equations describe the behaviour of electromagnetic systems in a macroscopic range, i.e., where quantum effects are excluded, see Box 2.1 for the case of resting media in space and time. This model is given by the interaction of electric $(\mathbf{E}, \mathbf{D})$ and magnetic fields $(\mathbf{H}, \mathbf{B})$ (1) and material laws (2). These equations are closed by appropriate initial and boundary values. They can be used to describe complex geometry settings and they include a wide range of spatial phenomena, e.g., skin effect, proximity effects, eddy currents, and so on. Thus Maxwell's equations (in various formulations) are used in the case of complex electric models. Applying such a field

Box 2.1: Maxwell's equations and material laws.

Differential equations:

$$\mathbf{curl}\,\mathbf{E} = -\frac{\partial \boldsymbol{B}}{\partial t}, \quad \mathbf{curl}\,\boldsymbol{H} = \frac{\partial \mathbf{D}}{\partial t} + \boldsymbol{J}, \quad \mathbf{div}\,\mathbf{D} = \rho, \quad \mathbf{div}\,\boldsymbol{B} = 0 \tag{1}$$

with *electric* and *magnetic field strength*: $\mathbf{E}$ and $\boldsymbol{H}$
electric and *magnetic flux density*: $\mathbf{D}$ and $\boldsymbol{B}$
current and *charge density*: $\boldsymbol{J}$ and ρ, respectively.

Material laws:

$$\mathbf{D} = \epsilon \mathbf{E}, \qquad \boldsymbol{H} = \frac{1}{\mu}\boldsymbol{B} = \nu \boldsymbol{B}, \qquad \boldsymbol{J} = \sigma \mathbf{E}, \tag{2}$$

with *permittivity* ϵ, *permeability* μ (*reluctivity* ν,) and *conductivity* σ.

description to an electric network both the interconnects and the elements are represented. Often for electric networks proximity effects as well as skin effects can often be neglected and the electric behaviour of can be reduced to the topology and lumped electric effects. This is called network model. The complexity of electric networks generally comes with the large scale integration. For such system with large scale integration a global field description of the network is even not neither feasible and not necessary.

2.2 Network Model from Maxwell's Equations

The network approach is based on integral quantities, where the three spatial dimensions of the physical circuit are only reflected by the topology of the network graph. All electrical behaviour is concentrated in ideal devices, which are ideally shunt (connected).

To mathematically describe electric networks, we have a set of basic elements, which have two terminals each (so-called one ports). This set typically comprises: resistances, capacitances, inductances, voltage and current sources. Each type of element describes a lumped electric effect (see below).

Now, let an electric network connect $n_I \in \mathbb{N}$ instances of these basic elements (by ideal conductors). For the electric behaviour it is important, which elements are connected (shunt). This gives a directed network graph, where each branch refers to a network element and each node identifies the electric shunt of certain attached elements. Let $n_u + 1$ denote the number of nodes, with one distinguished reference node (the ground node). Furthermore, each branch is directed to identify the positive direction electric current through the device. Thus we have two incidences for each branch: $+1$ and -1, with respect to the direction of the branch. Removing the incidences for the ground node, an incidence matrix $\boldsymbol{A} \in \{-1, 0\,1\}^{n_u \times n_I}$ describes the network topology.[1]

The transient behaviour of the network is described by *branch currents* $\boldsymbol{I}(t) \in \mathbb{R}^{n_I}$, *branch voltages* $\boldsymbol{U}(t) \in \mathbb{R}^{n_I}$ and *node potentials* $\boldsymbol{u}(t) \in \mathbb{R}^{n_u}$, the potentials with respect the ground node.

Assuming ideal conductors (connecting the basic network elements), ideal and concentrated nodes, stationary magnetic field ($\frac{\partial \boldsymbol{B}}{\partial t} = 0$), and stationary charge term ($\frac{\partial \rho}{\partial t} = 0$), the first two of Maxwell's equations

$$\mathbf{curl}\,\mathbf{E} = 0, \qquad \mathbf{div}\,\boldsymbol{J} = 0. \tag{3}$$

yield *Kirchhoff's laws*.

Kirchhoff's voltage law (KVL). Consider a loop (circle) formed by b conducting branches, see the schematic illustration Fig. 1a. The integration of (3_1) over the loop area A (singly connected) results in sum of path integrals:

$$0 = \oint_{\partial A} \mathbf{E} \cdot \mathbf{ds} = \sum_{j=1}^{b} \int_{\gamma_j} \mathbf{E} \cdot \mathbf{ds}.$$

Using branch voltages $U_j := \int_{\gamma_j} \mathbf{E} \cdot \mathbf{ds}$, $j = 1, \ldots, b$, it gives Kirchhoff's voltage law

$$\sum_{j=1}^{b} U_j = 0,$$

i.e., the sum of all branch voltages in a loop is always zero. In fact, this allows to introduce node potentials $\boldsymbol{u}$, such that

$$\boldsymbol{A}^\top \cdot \boldsymbol{u}(t) = \boldsymbol{U}(t). \tag{4}$$

Kirchhoff's current law. Consider a node with k branches (see Fig. 1b). Charge conservation (3_b), applied to a volume V engulfing this node yields by integration

[1] Notice, that the incidences of the ground node are still implicitly given.

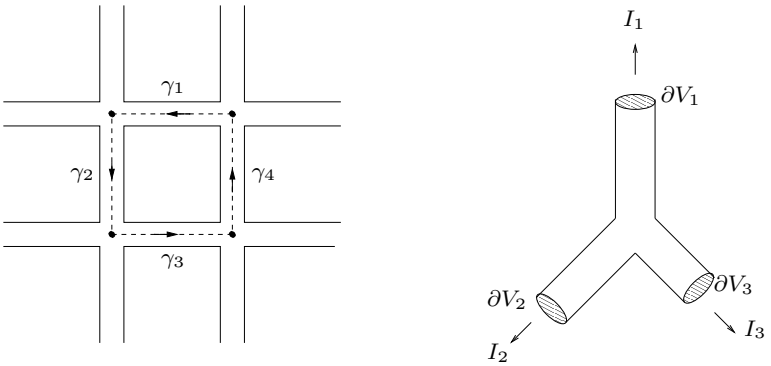

(a) Loop with four branches. (b) Node with $k = 3$ branches.

Fig. 1: Figures for Kirchhoff's laws.

$$0 = \int_{\partial V} \boldsymbol{J} \cdot \mathbf{dS} = \int_{\partial V_1} \boldsymbol{J} \cdot \mathbf{dS} + \ldots + \int_{\partial V_k} \boldsymbol{J} \cdot \mathbf{dS}.$$

By introducing the branch currents as integral quantities $I_i := \int_{\partial V_i} \boldsymbol{J} \cdot \mathbf{dS}$ $(i = 1, \ldots, k)$ finally Kirchhoff's current law is obtained

$$\sum_{j=1}^{k} I_i = 0.$$

I.e., in each node the sum of all inflowing branch currents is always zero:

$$\boldsymbol{A} \cdot \boldsymbol{I}(t) = 0, \tag{5}$$

with with incidence matrix $\boldsymbol{A}$ and $\boldsymbol{I}(t) \in \mathbb{R}^{n_I}$ denoting the vector of all branch currents.

Characteristic branch equations. Now for the state variables $\boldsymbol{I}$ and $\boldsymbol{u}$, we have the purely topological KCL (5). Thus we need additional n_I equations to define uniquely the state variables. Certainly, these equations have to describe the physical behaviour of the network elements — roughly as branch current/branch voltage relation. They are referred to as *characteristic branch equations.* Based on field theoretical arguments, the characteristic equations are derived from Maxwell's equations assuming quasistationarity. This gives the resistor for a concentrated Ohmic loss, the inductor for magnetic flux storage and the capacitor for charge storage. Each basic element disregards the other effects. Moreover these equations can be modelled linearly or nonlinearly. The basic family of one port elements is completed by independent, i.e., purely time-dependent current and voltage sources.

In this framework, complex elements such as semiconductors, are modelled by equivalent circuits which consist of basic elements and include often controlled sources, i.e., source terms, which depend on circuit quantities.

Modified nodal analysis (mathematical simulation model). Kirchhoff's laws, together with characteristic equations for all network elements, fully describe the electric network. Now, there are several ways to set up the mathematical model. Classically, electric networks (in circuit simulators) are formulated via modified nodal analysis (MNA), or its flux/charge oriented formulation, see e.g.

[31]. Thereby all node voltages are unknowns (KVL). KCL is used as balance equation for each node (except ground). All current defining elements are directly inserted and corresponding current variables are removed. If other quantities than node voltages are used for the current definition, branch relations have to be added. Similarly one needs to added the branch equations for all non-current defining elements to the system. In the end, one obtain the following set of unknowns: charges $q(t)$, fluxes $\phi(t)$, currents through inductances $i_{\mathrm{L}}(t)$, currents through voltage sources $i_{\mathrm{V}}(t)$ and all node potentials $u(t)$ except ground. These unknowns fulfill the following set of equations

$$A_{\mathrm{C}}\frac{\mathrm{d}}{\mathrm{d}t}q + A_{\mathrm{R}}g(A_{\mathrm{R}}^{\top}u,t) + A_{\mathrm{L}}i_{\mathrm{L}} + A_{\mathrm{V}}i_{\mathrm{V}} + A_{\mathrm{I}}i_{\mathrm{S}}(t) = 0, \tag{6a}$$

$$\frac{\mathrm{d}}{\mathrm{d}t}\phi - A_{\mathrm{L}}^{\top}u = 0, \qquad A_{\mathrm{V}}^{\top}u - v_{\mathrm{S}}(t) = 0, \tag{6b}$$

$$q - q_{\mathrm{C}}(A_{\mathrm{C}}^{\top}u,t) = 0, \qquad \phi - \phi_{\mathrm{L}}(i_{\mathrm{L}},t) = 0 \tag{6c}$$

with element specific incidences matrices $A_\star$ and element relations for capacitances $q_{\mathrm{C}}(v,t)$, resistances $g(v,t)$, inductances $\phi_{\mathrm{L}}(i,t)$, independent voltages sources $v_{\mathrm{S}}(t)$ and independent current sources $i_{\mathrm{S}}(t)$. Inserting the charge- and flux-defining relations into (6a) and (6b), we get

$$A_{\mathrm{C}}\frac{\mathrm{d}}{\mathrm{d}t}q_{\mathrm{C}}(A_{\mathrm{C}}^{\top}u,t) + A_{\mathrm{R}}g(A_{\mathrm{R}}^{\top}u,t) + A_{\mathrm{L}}i_{\mathrm{L}} + A_{\mathrm{V}}i_{\mathrm{V}} + A_{\mathrm{I}}i_{\mathrm{S}}(t) = 0, \tag{7a}$$

$$\frac{\mathrm{d}}{\mathrm{d}t}\phi_{\mathrm{L}}(i_{\mathrm{L}},t) - A_{\mathrm{L}}^{\top}u = 0, \tag{7b}$$

$$A_{\mathrm{V}}^{\top}u - v_{\mathrm{S}}(t) = 0. \tag{7c}$$

This charge-oriented model states a differential algebraic equation (DAE), which we address below.

2.3 DAE aspects of the network model and soundness of the network

Besides loops in the network, we need the notion of cutsets. These are minimal sets of branches, such that by removing these branches a given network is decomposed into a larger number of connected units. But removing only a proper subset, the connected units remain the same.

In the following it shall hold:

Assumption 2.1 (Soundness and local passivity, e.g. [11])

a) The network (overall) consists of a single connected unit and non-empty (i.e., at least one branch). There are neither loops of voltage sources only, nor cutsets of currents sources only, i.e., the following incidence matrices have full column rank:

$$A_V, \qquad [A_C\, A_R\, A_L\, A_V]^{\top}.$$

b) The network composed of is locally passive elements, i.e., the element functions q_{C}, ϕ_{L}, g are continuously differentiable and the Jacobians are positive definite:

$$\frac{\partial q_{\mathrm{C}}(v,t)}{\partial v}, \quad \frac{\partial \phi_{\mathrm{L}}(j,t)}{\partial j}, \quad \frac{\partial g(v,t)}{\partial v}$$

with corresponding variables (element-type respective branch currents j and branch voltages v).

Classically [24], we have for the tractability index [26]:

Theorem 2.2. *By Assumption 2.1, the charge-flux oriented network equations 7 are at least of index-1. Moreover the electric network model* (7) *is an index-1 DAE, if no CV-loop and no LI-cutset is present, otherwise index-2 — reformulated in terms of incidence matrices, this condition reads: the matrices*

$$(A_C, A_G, A_V)^\top, \quad Q_C^\top A_V$$

must have full column rank, with Q_C being a projector onto the kernel of A_C.

Remark 2.3.

a) For linear networks, the results coinside with the other index definitions as perturbations index (see [33] for index definitions).
b) This result can also be generalized to a rather general class of controlled current and voltage sources [24].

2.4 Further Reading

The network modelling introduced above for electrical networks is generally valid for flow networks, see e.g. Reinschke and Schwarz [46], and Jansen and Tischendorf [38]. Electrical currents and potentials generalize to flows and pressures in water, gas and blood flow networks. As for electrical networks, Kirchhoff's laws constitute topological relations between these flow and pressure quantities. As for electrical elements, water, gas and blood network element can be described in a static or dynamic way, both as lumped and distributed elements. If only lumped elements are involved, the network equations constitute DAE systems. If in addition distributed elements arise, one has to deal with PDAE network models. The latter will be discussed for the case of electrical networks in the next chapter. For water, gas and flow networks we refer, for example, to Quarteroni et al. [45], Engl [23] and Rentrop and Steinebach [43].

3 Modelling of Coupled Systems with Examples

Also due to downscaling, very large scale of integration and enhanced frequencies, electric circuits need to incorporate more and more former secondary effects. To include further effects, it is natural to enhance the network by more complex elements. This can be done via DAE models and PDE models. The PDE coupling is the more universal methodology, since we may add any possible physical effect via its natural description. Anyway, DAEs are obtained from a spatial discretization of any PDE model. Thus we distinguish between the following mechanisms:

(a) network-network coupling: subcircuits or companion models yield coupled DAE-DAE system. Lumped subcircuits can be fitted to model certain effects. Moreover on the circuit level, network models can be split up into subsystems to enable co-simulation.

(b) refined modelling: here, a PDE-model gives a current/voltage relation, such that the model fits seamless into the network. For the coupling a device current enters the current balances and the terminal node voltages enter the boundary condition of the PDE. We discuss refined models for semiconductor devices, magnetoquasistatic fields and transmission lines.
(c) multiphysics: here a further physical domain is added, which is described by a PDE. Coupling is not necessary via currents and voltages. We discuss thermal coupling.

In contrast to fitting lumped subcircuits in a DAE-DAE coupling, the PDAE coupling has always the advantage of describing physical effects directly using natural quantities. Furthermore it is important that these models fit into circuit design, i.e., can be automatically generated, fit to the network DAE modelling and simulation approach.

We begin with network coupling, then follow semiconductors , transmission lines, heat and magnetoquasistatic models.

3.1 Electric Networks Coupled to Electric Networks

In the following we discuss circuit partioning and a semi-explicit representation for analysis purposes.

Partioning

The design process of large integrated circuits is based on circuit partitioning. This may be regarded as domain decomposition techniques applied already at the modelling level: subcircuits of different functionality are modelled independently, possibly by different experts using different CAD tools; in the end, these subsystems have to be assembled into one overall system; this is done by connecting their terminals (see Fig. 2, left). From an electrical point of view, this coupling procedure can be described by introducing virtual voltage sources as coupling units at the boundaries (see Fig. 2, right). In this context, virtual means that $v(t) = 0$, and thus the nodes share the same node potentials.

For r subsystems, we have r instances of the network equations (7):

$$0 = A_{C_i}\frac{d}{dt}\left[q_i(A_{C_i}^\top u_i, t)\right] + A_{G_i} g_i(A_{G_i}^\top u_i, t) + A_{L_i}\jmath_{L_i} + A_{V_i}\jmath_{V_i} + A_{I_i}\imath_i(t) \tag{8a}$$

$$0 = \tfrac{d}{dt}\left[\phi_i(\jmath_{L_i}, t)\right] - A_{L_i}^\top u_i \tag{8b}$$

$$0 = A_{V_i}^\top u_i - v_i(t) = 0 \qquad (i = 1, \ldots, r) \tag{8c}$$

with node voltages $u_i(t) \in \mathbb{R}^{n_{u_i}}$ and branch currents $\jmath_{V_i}/\jmath_{L_i}$ through voltage/flux sources for the i-th subcircuit. For the coupling of the subnetworks, we assume to have overall n_u coupling branches with branch currents $\lambda(t) \in \mathbb{R}^{n_i}$. Moreover $A_{\lambda_i} \in \{-1, 0, 1\}^{n_{u_i} \times n_u}$ shall denote the incidence matrix of the coupling branches (virtual voltage sources) with the $i-$th subsystem. Then the coupling is twofolded:

- *contribution to KCL:* the coupling currents are added to the current balances at the coupling nodes: $A_{\lambda_i}\lambda$. Hence we can give the update of A_I:

$$A_{I_i} \rightsquigarrow (A_I,\, A_{\lambda_i})\,, \quad \imath_i \rightsquigarrow \begin{pmatrix} \imath_i \\ u \end{pmatrix}.$$

- *identification of node potentials:* the node potentials of two connected subsystems have to coincide at the boundaries (virtual voltage sources). This gives an additional coupling equation (9c), see below.

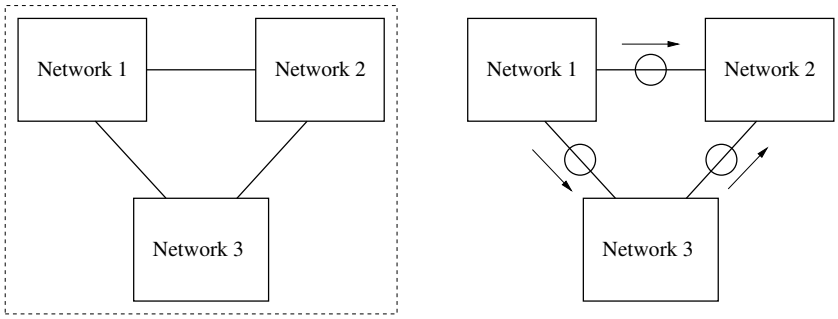

Fig. 2: Distributed modelling of networks

Summing up, we have for r coupled DAE network models:

$$\begin{aligned} 0 &= A_{C_i} \frac{d}{dt}\left[q_i(A_{C_i}^\top u_i, t)\right] + A_{G_i} g_i(A_{G_i}^\top u_i, t) + A_{L_i} \jmath_{L_i} + A_{V_i} \jmath_{V_i} + \\ &\quad + A_{I_i} \imath_i(t) + A_{\lambda_i} \lambda \qquad (9a) \\ 0 &= \tfrac{d}{dt}\left[\phi_i(\jmath_{L_i}, t)\right] - A_{L_i}^\top u_i \qquad (9b) \\ 0 &= A_{V_i}^\top u_i - v_i(t) = 0 \qquad (i = 1, \ldots, r) \qquad (9c) \end{aligned}$$

with linear coupling equations

$$0 = \sum_{i=1}^{r} A_{\lambda_i}^\top \cdot u_i \qquad (9d)$$

Defining $x_i := (u_i^\top, \jmath_L^\top, \jmath_V^\top)^\top$ and $s_i := (q_i^\top, \phi_i^\top)^\top$, the partitioned DAE network systems (9a) are of linear-implicit form

$$0 = \mathcal{F}_i\,(x_i, \dot{y}_i, \lambda) \;\; \text{with} \;\; y_i := s_i(x_i) \;\; \text{and} \;\; A_i := \partial \mathcal{F}_i / \partial \dot{y}_i \equiv \text{const}, \qquad (10a)$$

$i = 1, \ldots, r$, with the linear boundary condition (9d) being a special case of an algebraic coupling condition

$$0 = \mathcal{G}(x_1, \ldots, x_r)\,. \qquad (10b)$$

Semi-Explicit Formulation

For the analysis and cosimulation study, a semi-explicit formulation is helpful:

Lemma 3.1. *It is possible to transfer the linear-implicit non-Hessenberg system (9a–9c) into a semi-explicit DAE systems of the type*

$$\left.\begin{aligned} \dot{y}_i(t) &= f_i(y, z_i, \lambda) \\ 0 &= h_i(y, z_i, \lambda) \end{aligned}\right\} \qquad (i = 1, \dots, r) \tag{11a}$$

that are coupled by algebraic equations

$$0 = g(y, z)\ . \tag{11b}$$

Proof. Let Q_{V-C_i} denote the projector onto $\ker A_{V_i}^\top Q_{C_i}$, and $P_{V-C_i} := I - Q_{C_i}$ be its complementary projector, the node potentials u_i of the i-th subsystem can be written as

$$u_i = P_{C_i} u_i + Q_{C_i} P_{V-C_i} u_i + Q_{C_i} Q_{V-C_i} u_i.$$

By introducing $z_i^\top := ((P_{C_i}u_i)^\top,\ \jmath_{L_i}^\top,\ (Q_{C_i}P_{V-C_i}u_i)^\top,\ (Q_{C_i}Q_{V-C_i}u_i)^\top,\ \jmath_{V_i}^\top)$, the system (9) can be transformed into the semi-explicit index-1 system (11):

$$f_i^\top = (f_{i,1}^\top, f_{i,2}^\top), \quad h_i^\top = (h_{i,1}^\top, \dots, h_{i_4}^\top),$$

where $f_{i,1}, f_{i,2}, h_{i,1}, \dots, h_{i_4}$ are defined as

$$\begin{aligned}
f_{i,1} &= P_{C_i}^\top \big(A_{R_i} r_i(A_{R_i}^\top(z_{i,1}+z_{i,3}+z_{i,4}), t) + A_{L_i} z_{i,2} + A_{V_i} z_{i,5} + A_{I_i} \imath_i(t) + A_{\lambda_i}\lambda\big) \\
f_{i,2} &= -A_{L_i}^\top (z_{i,1} + z_{i,3} + z_{i,4}), \\
h_{i,1} &= y_i - \begin{pmatrix} A_{C_i} q_i(A_{C_i}^\top z_{i,1}, t) + Q_{C_i}^\top Q_{C_i} z_{i,1} \\ \varphi_{L_i}(z_{i,2}, t) \end{pmatrix} \\
h_{i,2} &= Q_{C_i}^\top A_{V_i} A_{V_i}^\top (z_{i,1} + z_{i,3}) - v_i(t) \\
h_{i,3} &= Q_{V-C_i}^\top Q_{C_i}^\top \big(A_{R_i} r_i(A_{R_i}^\top(z_{i,1}+z_{i,3}+z_{i,4}), t) + A_{L_i} z_{i,2} + A_{I_i} \imath_i(t) + A_{\lambda_i}\lambda\big) \\
h_{i,4} &= A_{V_i}^\top Q_{C_i} P_{V-C_i}^\top Q_{C_i}^\top \big(A_{R_i} r_i(A_{R_i}^\top(z_{i,1} + z_{i,3} + z_{i,4}), t) + A_{L_i} z_{i,2} + A_{V_i} z_{i,5} \\
&\qquad + A_{I_i} \imath_i(t) + A_{\lambda_i}\lambda\big)
\end{aligned}$$

and with coupling condition

$$g = \sum_{i=1}^{r} A_{u_i}^\top (z_{i,1} + z_{i,3} + z_{i,4}). \qquad \square$$

We will come back to this semi-explicit formulation in Section 5.

Remark 3.2. One may introduce splitting matrices P_i $(i = 1, \dots, r)$ to define a parts of the coupling condition $P_i\mathcal{G}$ for each subsystem, where these part may have an overlapping. This results in r coupled DAE system of the type

$$0 = \widetilde{\mathcal{F}}_i(x_i, \dot{y}_i, u, \bar{\lambda}_i) \qquad (i = 1, \dots, r)$$

with $\bar{\lambda}_i = P_i^\top u$. For more details see [2, 9].

3.2 Electric Networks Coupled to Distributed Semiconductor Devices

We present the 1D PDAE diode network model from [3]. Given an electrical network which contains semiconductor devices with two Ohmic contacts such as a diodes, we assume that a spatially 1D diode model is sufficient to describe its behavior. Thus for such reduced model we have a doping profile $C(x)$ on a line segment $x \in (0, l) \subseteq \mathbb{R}$. We disregard thermal effects and assume that both electrons and holes generate the diode's current densities for electrons j_n and holes j_p. To this end, let $n = n(x,t)$ and $p = p(x,t)$ be the number densities of electrons (with negative charge $-q$) and holes (with positive charge q). Furthermore let $V = V(x,t)$ be the electrostatic potential (in the diode). Then the evolution of the number densities and the potential is given by the drift-diffusion system (16a), see Box 3.1, which states the diode's behavior, see also [41]. The occurring parameters are: $R = R(n,p)$ denotes the recombination-generation term, $\mu_n > 0$ and $\mu_p > 0$ denote mobilities (for electrons and holes) and U_T refers to the thermal potential.

For the initial profile we have positive functions $p_0, n_0 \in L^2([0,l])$ given:

$$n(x,0) = n_0(x), \quad p(x,0) = p_0(x), \tag{12a}$$

and boundary conditions are inferred from the doping profile C resulting in n_D, p_D (see [41])

$$n(x,t) = n_D(x), \quad p(x,t) = p_D(x), \qquad x = 0, l, \tag{12b}$$

the built-in potential V_{bi} and applied voltage drop $v_D = v_D(t)$ result in the boundary condition:

$$V(0,t) = V_{\mathrm{bi}}(0) \quad V(l,t) = V_{\mathrm{bi}}(l) + v_D(t) \tag{12c}$$

For further details see also [41, 49, 3].

Coupling conditions

We consider a network with one diode for simplicity of presentation and let $\boldsymbol{A}_D$ denote the diodes network incidence matrix. From the perspective of the electric network, the drift-diffusion system (16a) defines a PDE current-voltage relation. Thus is coupled to the network variables as follows. The voltage drop v_m is defined from the electric network variables,

$$v_D = u_2(t) - u_1(t) = \boldsymbol{A}_D^\top \boldsymbol{u}(t), \tag{13}$$

while the diode's current I_D enters the KCL according to the network topology given by the incidence matrix $\boldsymbol{A}_D$ as summand $\boldsymbol{A}_D I_D$. The current I_D itself is obtained from conservation of charge (from the evolution equations for n and p)

$$\partial_t(-qn + qp) + \partial_x J = 0.$$

Inserting the Poisson equation for $(-qn + qp)$, we find that $-\epsilon \partial_t \partial_x V(x,t) + J(x,t)$ is constant over $(0,l)$. Thus by taking the average, the device current can be assigned as [3]

Box 3.1: Standard mixed system (network-diode) - Version I .

Parabolic-elliptic problem for the diode:

$$\begin{aligned} -q\partial_t n + \partial_x j_n = qR, \qquad & j_n = -q\left(\mu_n n \partial_x V - U_T \mu_n \partial_x n\right), \\ q\partial_t p + \partial_x j_p = -qR, \qquad & j_p = -q\left(\mu_p p \partial_x V + U_T \mu_p \partial_x p\right), \\ -\epsilon\,\partial_x^2 V = q(C - n + p), & \\ V(0,t) = V_{\rm bi}(0), \quad V(l,t) = V_{\rm bi}(l) + v_D(t), & \quad \text{(plus BCs and IVs)} \end{aligned} \tag{16a}$$

Coupling interface:

$$v_D = u_2 - u_1 = \boldsymbol{A}_D^\top \boldsymbol{u}, \qquad I_D(t) = -\epsilon \partial_t \partial_x V(x,t) + J(x,t), \tag{16b}$$

DAE-IVP problem for the network: given by DAE (7) plus updating:

$$A_I \rightsquigarrow (A_I \quad A_D) \qquad \imath(t) \rightsquigarrow \begin{pmatrix} \imath(t) \\ I_D(t) \end{pmatrix} \tag{16c}$$

$$I_D(t) = -\frac{\epsilon}{l}\frac{\mathrm{d}}{\mathrm{d}t}(u_2(t) - u_1(t)) + \langle J \rangle(t) = \frac{\epsilon}{l}\boldsymbol{A}_D^\top \frac{\mathrm{d}\boldsymbol{u}}{\mathrm{d}t} + \langle J \rangle(t), \tag{14}$$

leading to the KCL summand

$$\boldsymbol{A}_D I_D = \frac{\epsilon}{l}\boldsymbol{A}_D \boldsymbol{A}_D^\top \frac{\mathrm{d}\boldsymbol{u}}{\mathrm{d}t} + \boldsymbol{A}_D \langle J \rangle . \tag{15}$$

Now, (15) gives rise for two coupling versions: First, we compute from the diode I_D (14) and stamp it via (15) into KCL. This is given in Box 3.1. On the other hand, the first term in (15) resembles a capacitance, which depends only on the network and gives rise to a modified capacitance matrix and a remaining coupling current (the averaging term). This is stated in Box 3.2. In structural terms of the electric network, the diode behaves as a controlled current source with a parallel capacitance.

In the stationary case, where the time derivative of the number densities are disregarded [41, 4], the parabolic-elliptic IBVP above transforms to an elliptic BVP. Note that in this case the dynamic current contribution $(\epsilon/l)A_D^\top A_D \dot{u}$ (capacitance term) disappears and only the static current contribution $A_D \langle J \rangle$ remains. Thus, the current $\langle J \rangle(.)$ denotes the static response of an applied voltage drop (in Box 3.1 and Box 3.2). Hence in this case, the models in both boxes coincide.

Remark 3.3. Notice that the coupling slightly differs from previous works: we couple only via branch voltages and branch currents. Node voltages are not needed, since the semiconductor model (and also any network model) must be invariant under a change of the ground voltage.

Further generalization from a 1D spatial model to multiple dimensions are found e.g. in [5, 7] and to devices with more than two contacts in [1].

Box 3.2: Standard mixed system (network-diode) - Version 2 .

Parabolic-elliptic problem for the diode:

$$\text{standard drift-diffusion system, see (16a).} \tag{17a}$$

Coupling interface:

$$v_D = u_2 - u_1 = \boldsymbol{A}_D^\top \boldsymbol{u}, \qquad \langle J \rangle = \langle j_n + j_p \rangle; \tag{17b}$$

DAE-IVP problem for the network: given by DAE (7) plus updating:

$$\begin{aligned} A_C &\rightsquigarrow (A_C \quad A_D) & A_I &\rightsquigarrow (A_I \quad A_D) \\ q_C(A_C^\top u, t) &\rightsquigarrow \begin{pmatrix} q_C(A_C^\top u, t) \\ \frac{\epsilon}{l} A_D^\top u \end{pmatrix} & \imath(t) &\rightsquigarrow \begin{pmatrix} \imath(t) \\ \langle J \rangle \end{pmatrix} \end{aligned} \tag{17c}$$

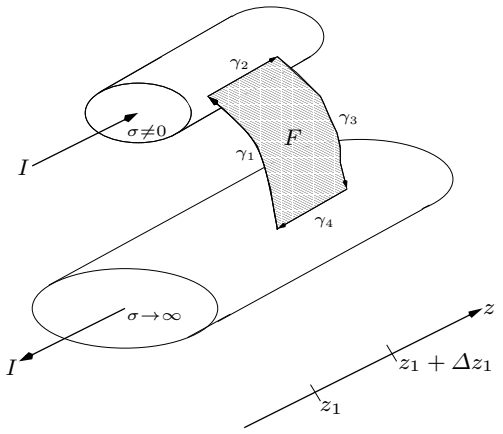

Fig. 3: Sketch of a lossy transmission line with supply ($\sigma \neq 0$) and return ($\sigma \to \infty$) conductor (which is ground).

3.3 Electric Network Coupled to Telegraphers Equation

In the network approach, the interconnects are ideal such that they amount to pure topological conditions. Due to high integration rate and reduced clock time in many of today's applications, the propagation of signals, dispersion, reflection and electromagnetic coupling are parasitic effects of the interconnect system. These effects may lead to delay, crosstalk and multiple switching in digital circuits. And thus they need to be modelled on top to guarantee functionality.

One aims at including interconnect effects up to a necessary level to enhance accuracy, but without unnecessarily increasing the simulation effort. Thus one finds the full range from lumped companion models up to 3d descriptions using full Maxwell's equations (1-2).

Following the lines of [29], we discuss an appropriate model between 0d and 3d. Fig. 3 illustrates a lossy transmission line with supply and return conductor on an integrated circuit. The latter models propagating signals of arbitrarily low frequency in digital circuits. The regular structure of transmission lines on chips allows for some simplifying assumptions, which lead to a $1d$ model [27]:

1. *No skin effect.* In integrated circuits, the skin effect (for a lossy conductor) can be disregarded. Thus the current density is homogeneous (perpendicular to the signal propagation), and we obtain the line current (with cross section area $|S(z)|$)
$$I(z,t) := \int_{S(z)} \boldsymbol{J} \cdot \mathbf{dS} = J_3(z,t)|S(z)|, \quad \boldsymbol{J} = (J_1\,, J_2\,, J_3)^\top.$$
2. *Quasistationary behaviour transversal to the direction of propagation.* Assuming a quasistationary behaviour transversal to the direction of propagation, the magnetic field component in propagation direction (here $\mathbf{H}_z$) is constant in time. Hence for any plane perpendicular to the direction of propagating, Maxwell's equation (1a) yields
$$\mathbf{curl}\,\mathbf{E}\Big|_{z\,=\,\mathrm{const}} = -\frac{\partial \boldsymbol{B}}{\partial t}\Big|_{z\,=\,\mathrm{const}} = 0, \tag{18}$$
i.e., $\mathbf{E}$ defines a potential restricted to z =const. Hence for constant z a path γ connecting the conductor's surface with the return conductor
$$V(z,t) := \int_\gamma \mathbf{E} \cdot \mathbf{ds}, \qquad (\gamma \text{ with constant } z) \tag{19}$$
is independent of the path.
3. *Linear materials.* Assuming linear materials (and quasistationarity), the charge density (per unit length) Q_z is proportional to the line voltage V
$$Q_z(z,t) = C(z) \cdot V(z,t) \quad \text{with} \quad Q_z(z,t) := \int_{S(z)} \rho\, dS(z), \tag{20}$$
the flux density (per unit length) Φ_z is proportional to the line current I
$$\Phi_z(z,t) = L(z) \cdot I(z,t) \quad \text{with} \quad \Phi_z(z,t) := \lim_{\Delta z \to 0} \frac{1}{\Delta z} \int_F \boldsymbol{B} \cdot \mathbf{dF} \tag{21}$$
The constants C and L are referred to as *capacitance* and *inductance per unit length*, and $R(z) := 1/(\sigma|S(z)|)$ *resistance per unit length.*

Based on these three assumptions, Maxwell's equations yield a transmission line model in terms of line voltage and line current: the telegrapher's equations.

Maxwell's first law (1a) yields by integration (see Fig. 3)
$$\oint_{\partial F} \mathbf{E} \cdot \mathbf{ds} = -\int_F \boldsymbol{B}_t \cdot \mathbf{dF}.$$

From (18-19) we obtain for the terms on the left-hand side

$$\int_{\gamma_1} \mathbf{E}\cdot\mathbf{ds} = -V(z_1,t), \qquad \int_{\gamma_2} \mathbf{E}\cdot\mathbf{ds} = \int_{z_1}^{z_1+\Delta z} \frac{I(z,t)}{\sigma|S(z)|}\,dz,$$
$$\int_{\gamma_3} \mathbf{E}\cdot\mathbf{ds} = V(z_1+\Delta z,t), \qquad \int_{\gamma_4} \mathbf{E}\cdot\mathbf{ds} = 0.$$

Taking the limit $\Delta z \to 0$ we find

$$V_z(z,t) + L(z)I_t(z,t) + R(z)I(z,t) = 0. \tag{22}$$

where the right-hand side uses (21). Furthermore charge conservation $\rho_t + \mathbf{div}\,\boldsymbol{J} = 0$ (which follows from Maxwell's equations (1)) yields on the interval z_1 and $z_1 + \Delta z$

$$\int_{z_1}^{z_1+\Delta z_1} \frac{d}{dt}\big(Q_z(z,t)\big)\mathrm{d}z + (I(z_1+\Delta z,t) - I(z_1,t)) = 0,$$

and thus in the limit $\Delta z \to 0$ together with (20) we deduce

$$C(z)V_t(z,t) + I_z(z,t) = 0. \tag{23}$$

Given d interconnects of length l each, we have d-dimensional line quantities ($\boldsymbol{V}(z,t)$, $\boldsymbol{I}(z,t)$) and symmetric positive-definite capacitance and inductance matrices $\boldsymbol{L}(z)$, $\boldsymbol{C}(z)$ (defining mutual capacitance and inductance) and a diagonal positive-semidefinite $\boldsymbol{R}(z)$ (resistance matrix). Thus (22–23) yield the system of telegrapher's equations (24a) (Box 3.3). For transmission lines on integrated circuits, one can assume $\boldsymbol{C}$, $\boldsymbol{L}$, and $\boldsymbol{R}$ to be independent of z.

System (24a) is a first order linear hyperbolic model. It is completed by initial values and boundary conditions, which come from node potentials of the attached network. That is, let $\boldsymbol{A}_\lambda$ denote the incidence matrix [2] for the d transmission lines, then $\boldsymbol{A}_\lambda^\top u = (u_1 - u_{\text{ground}}, u_2 - u_{\text{ground}}) = (u_1, u_2)$ gives the applied voltage differences at both ends — here we have set the ground potential u_{ground} to zero. The transmission lines outputs the branch currents λ, which enter KCL: $\boldsymbol{A}_\lambda\lambda$ (where $\lambda := (\lambda_1, \lambda_2)^\top$). This completes the network model given in Box 3.3 [29].

3.4 Electric Networks Coupled to Magnetoquasistatic Fields

In Section 3.3 we have incorporated distributed, quasi-stationary and inductive effects of transmission lines into the network approach using a model reduction approach based on integral quantities such as line currents and line voltages. Here, we discuss a more general case, where one cannot reduce the spatial complexity to 1D, but a detailed geometry is necessary, as it is the case for inductive machines. This yields the magnetoquasistatic conductor network model [52], which we present next.

To this end, we revisit Maxwell's equations (1) and assume that the time-variations of the electric fields (with respect to time) are small compared to the current density. This amounts to

[2] This matrix defines already, as in the previous cases, a reduced incidence matrix: the ground potential $u_{\text{ground}} = 0$ is not an unknown state variable, as the current law for the ground is not part of the network equations.

Box 3.3: Standard mixed system (network - lossy transmission line).

Hyperbolic IVP for lossy transmission line (Telegrapher's equations):

$$0 = \begin{pmatrix} \boldsymbol{C}\boldsymbol{V}_t(z,t) + \boldsymbol{I}_z(z,t) \\ \boldsymbol{L}\boldsymbol{I}_t(z,t) + \boldsymbol{V}_z(z,t) + \boldsymbol{R}\boldsymbol{I}(z,t) \end{pmatrix}, \tag{24a}$$

$$\begin{pmatrix} \boldsymbol{V}(0,t) \\ \boldsymbol{V}(l,t) \end{pmatrix} = \begin{pmatrix} u_1(t) \\ u_2(t) \end{pmatrix} \qquad \text{(plus IVs)} \tag{24b}$$

Coupling interface:

$$\begin{pmatrix} u_1(t) - u_{\text{ground}} \\ u_2(t) - u_{\text{ground}} \end{pmatrix} = \boldsymbol{A}_\lambda^\top \boldsymbol{u}(t), \qquad \lambda(t) = \begin{pmatrix} \boldsymbol{I}(0,t) \\ -\boldsymbol{I}(l,t) \end{pmatrix}. \tag{24c}$$

DAE-IVP problem for the network: given by DAE (7) plus updating:

$$A_I \rightsquigarrow (A_I \quad A_\lambda) \qquad \imath(t) \rightsquigarrow \begin{pmatrix} \imath(t) \\ \lambda(t) \end{pmatrix} \tag{24d}$$

the assumption $\frac{\partial \mathbf{D}}{\partial t} = 0$ and is referred to as magnetoquasistatics (MQS). Clearly, it holds for low frequency applications, which we consider here.

Often Maxwell's equations are used in terms of the so-called magnetic vector potential $\mathbf{A}$ and the scalar potential ϕ, implicitly defined by

$$\mathbf{B} = \mathbf{curl}\,\mathbf{A}, \qquad \mathbf{E} = -\frac{\partial \mathbf{A}}{\partial t} - \mathbf{grad}\,\phi. \tag{25}$$

Using the material relations $\mathbf{H} = \nu\mathbf{B}$ and $\mathbf{J} = \sigma\mathbf{E}$ to replace $\mathbf{H}$ and $\mathbf{B}$ in Ampère's law (1_2) and inserting the magnetic vector potential, we obtain the so-called curl-curl equation:

$$\sigma\frac{\partial \mathbf{A}}{\partial t} + \mathbf{curl}\,(\nu\,\mathbf{curl}\,\mathbf{A}) = -\sigma\,\mathbf{grad}\,\phi. \tag{26}$$

The choice of variables in this setup is not unique and several other formulations exist (e.g. [14]). We note that an integrable $\mathbf{B}$ defines $\mathbf{A}$ up to a gradient field. Therefore a unique solution requires a so-called gauging condition. One example is the Coulomb gauge: $\mathbf{div}\,\mathbf{A} = 0$. An alternative is to regularize the curlcurl operator in (26):

$$\mathbf{curl}\,(\nu\,\mathbf{curl}\,\mathbf{A}) \rightsquigarrow \mathbf{curl}\,(\nu\,\mathbf{curl}\,\mathbf{A}) + \mathcal{Y}\mathbf{A},$$

such that $\mathcal{Y}$ is positive definite on $\ker(\sigma)$ and zero elsewhere.

Since this model (26) will be coupled to electric networks, and coupling is confined to some finite domain Ω, boundary conditions have to be supplied. We assume Dirichlet and Neumann parts: $\Gamma = \Gamma_{\text{dir}} \cup \Gamma_{\text{neu}}$, where we assign:

$$\begin{aligned} &\mathbf{A} \times \mathbf{n} = \mathbf{A}_{\text{dir}} \quad \text{on } \Gamma_{\text{dir}} \\ &\nu\,(\mathbf{curl}\,\mathbf{A}) \times \mathbf{n} = \mathbf{H}_{\text{neu}} \quad \text{on } \Gamma_{\text{neu}} \end{aligned}$$

for the outer normal $\mathbf{n}$ and given $\mathbf{A}_{\mathrm{dir}}$, $\mathbf{H}_{\mathrm{neu}}$. Last initial values are assigned:

$$\mathbf{A}(t,\mathbf{r}) = \mathbf{A}(0,\mathbf{r}) \quad \text{for } \mathbf{r} \in \overset{\circ}{\Omega}\,.$$

Again such a PDE model is the right way to assign distributed data (e.g. ν, geometry) directly. Often these devices are coupled to an electric circuit. Thus they occur as submodel and we refer to this submodel as MQS device.

Circuit Coupling

Attaching an electric circuit to an MQS device results in an external current source for the curl-curl equation. This coupling current can only occur on some conducting subset $\Omega_M \subseteq \Omega$ of the MQS device. To model a single conductor, we assume Ω_M to be connected. Thus on Ω_M the scalar potential $\mathbf{\Phi}$ must be related to the applied voltage drop v_{M}. Furthermore the current density must be related to the respective branch current i_{M} of the electric circuit via integration.

As in [52], we consider a (connected) piece of a solid conductor (see Fig. 4) with two contacts

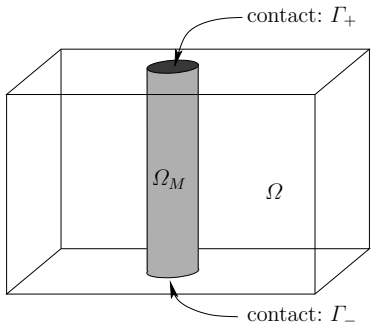

Fig. 4: MQS coupling in space [34].

Γ_+ and Γ_-, which are perfectly conducting. Since the corresponding network shunts are lumped, these connections have no field contributions (i.e., these effects are disregarded), [34]. Let γ denote a path connecting Γ_+ and Γ_- inside of Ω_M. Together with the applied voltage v_{M}, a closed loop is formed which incloses the area A_γ. Integration of Faraday's law (1_1) yields [52]

$$\int_\gamma \mathbf{E}\cdot \mathrm{d}\mathbf{s} - v_{\mathrm{M}} = -\frac{d}{dt}\int_{A_\gamma} \mathbf{B}\cdot \mathrm{d}\mathbf{A} \quad \Leftrightarrow \quad v_{\mathrm{M}} = -\int_\gamma \mathbf{grad}\ \phi \cdot \mathrm{d}\mathbf{s},$$

using the definition of the magnetic vector potential (25). To impose a lumped circuit voltage drop v_{M} onto the domain Ω_M, we use the linearity of Ohm's law, which allows us to treat the case of a unit excitation (i.e., $v_{\mathrm{M}} = 1$, [21, 52]). One can drive a Poisson problem from Maxwell's equations for the scalar potential ϕ^*:

$$\mathbf{div}\,\sigma\mathbf{grad}\ \phi^* = 0 \quad \text{with} \quad \phi^*|_{\Gamma_+} = 1, \quad \phi^*|_{\Gamma_-} = 0, \quad \mathbf{grad}\ \phi^*\cdot\mathbf{n} = 0 \ \text{ on } \Gamma_N,$$

where Γ_N is boundary of Ω_M without the contacts, $\mathbf{n}$ is the outer normal. Its solution ϕ^* yields a distribution function

$$\chi_{\mathrm{M}} := -\mathbf{grad}\ \phi^*,$$

which just depends on the geometry of the conductor's shape Ω_M. Thus χ_{M} can be computed in advanced for a given setting. Now, to have an applied voltage of v_{M}, we have just to scale this contribution by v_{M}. Thus the source term for the curl-curl equation (26) reads: $-\sigma\mathbf{grad}\,\phi = \sigma \cdot \chi_{\mathrm{M}} \cdot v_{\mathrm{M}}$, which gives the model (27a), see Box 3.4.

For the coupling, the voltages drop is deduced from the corresponding node potentials: network $v_{\mathrm{M}} = A_{\mathrm{M}}^{\top} u$ (with corresponding incidence matrix A_{M}). And furthermore, as total device current we average the current with respect to χ_M (on Ω_M):

$$\begin{aligned} i_M &:= \int_{\Omega_M} \chi_M\, \boldsymbol{J}\, \mathrm{d}\mathbf{r} = \int_{\Omega_M} \chi_M\, \mathbf{curl}\,(\mathbf{H})\, \mathrm{d}\mathbf{r} \\ &= \int_{\Omega_M} \chi_M\, \mathbf{curl}\,\left(\nu\, \mathbf{curl}\,(\mathbf{A})\right)\, \mathrm{d}\mathbf{r}. \end{aligned}$$

(using Ampère's law (1_2), magnetic vector potentials and the curlcurl equation).

Remark 3.4. In general, MQS devices are multiports; e.g. a transformer consisting of two coils. In this case, we need to define a distribution function for each electrical branch as above, where we have disjoint conducting subdomains.

Box 3.4: MQS-Coupling.

MQS device (Curl-Curl equation):

$$\sigma \frac{\partial \mathbf{A}}{\partial t} + \mathbf{curl}\,(\nu\, \mathbf{curl}\, \mathbf{A}) = \sigma\, \chi_M v_M \tag{27a}$$

Coupling conditions:

$$v_{\mathrm{M}} = A_{\mathrm{M}}^{\top} u, \qquad i_M = \int_{\Omega} \chi_M \mathbf{curl}\,(\nu\, \mathbf{curl}\, \mathbf{A})\, \mathrm{d}\mathbf{r} \tag{27b}$$

DAE-IVP problem for the network: given by DAE (7) plus updating:

$$A_I \rightsquigarrow (A_I \quad A_M), \qquad \imath(t) \rightsquigarrow \begin{pmatrix} \imath(t) \\ i_M(t) \end{pmatrix} \tag{27c}$$

3.5 Electric Network Coupled to Heat Transport

Power densities in electric circuits become more and more important, also due to downscaling, where more and more devices are packed on the same area [47]. Hence, circuit design needs to be equipped with thermal models that resolve the thermal aspect. There are already several approaches: starting

from heat networks [25], where heat is modeled only as a lumped quantity and a corresponding thermal network is fitted [28, 35]); up to distributed models [10, 19, 20], which involve directly the geometric layout (to address only a few approaches).

We consider an electric network model where some part is tightly thermally coupled. For instance, image a die where multiple semiconductor elements (transistors, diodes) share the same substrate. Due to resistive losses of the currents through the semiconductor, the substrate heats up and corresponding neighboring elements are heated indirectly.

To model such a coupled system, we need to introduce the domain $\Omega \subseteq \mathbb{R}^2$, where the temperature field T is recognised. For simplicity, we restrict our description to 2D (1D is possible, see [10], 3D is analog). Let the number of thermally relevant electric device be $n_T \in \mathbb{N}$ and let the kth element fill the space $\Omega_k \subseteq \Omega$. Since circuit simulators operate on lumped quantities for each device, we deduce a lumped device temperature θ_k by averaging [10, 20]:

$$\theta_k = \frac{1}{|\Omega_k|} \int_{\Omega_k} T d\Omega. \tag{28}$$

Now, a thermally active device dissipates power $p_k = p_k(\mathbf{u}, \boldsymbol{\theta})$ due to resistive losses. This yields a source term of the heat conduction (29a), where heat capacity c, heat conductivity λ, heat exchange with environment γT ($\gamma > 0$) and indicator function $\mathbf{1}_{\Omega_k}$ of Ω_k are used. In this way the power p_k is equally distributed on the device domain Ω_k.

Box 3.5: Network Heat Model.

Heat Diffusion:

$$c\frac{\partial T}{\partial t} - \lambda \Delta T + \gamma T = \sum_k \frac{p_k(\mathbf{u}, \boldsymbol{\theta})}{|\Omega_k|} \mathbf{1}_{\Omega_k} \tag{29a}$$

Coupling: dissipated power (p_k), lumped temperature (θ_k)

$$p_k = p_k(\mathbf{u}, \boldsymbol{\theta}) \qquad \theta_k = \frac{1}{|\Omega_k|} \int_{\Omega_k} T d\Omega \tag{29b}$$

Network DAE: (update)

$$G \rightsquigarrow G(\theta) \tag{29c}$$

In fact Joule law gives the dissipated power (for a linear resistance):

$$p_k = u_k \cdot \imath_k = \frac{1}{R} u_k^2,$$

where u_k denotes the branch voltage, $\imath_k$ the respective branch current and R the resistance (Ohm's Law).

Furthermore, one needs to couple heat to the network. This is done via parameters of the network. The basic parameter is the resistance, which increases with the corresponding lumped temperature θ [10]:

$$R = \rho_0 \cdot (\theta + \beta\theta^2),$$

with material parameters $\rho_0, \beta \geq 0$. Of course, this also applies to nonlinear resistances, e.g. as diodes, where temperature changes also the mobility of the carriers.

The new aspect of this multiphysical coupling summarized in Box 3.5 is, that the electric network depends on temperature T only via parameters. This is different to the above discussed settings of refined network modelling. Here it is important to model also the basic elements with a thermal layer. Moreover, the network topology (based on incidence matrices) is not enough to describe heat conduction, but the geometric positions of the thermally active elements are needed.

4 Analytical Properties of the Coupled Models

For PDAEs in refined electrical network modelling some analytical results are available: we have existence and uniqueness results for special hyperbolic, elliptic and parabolic PDAE systems arising when coupling circuits with transmission lines, stationary and instationary diode models, e.g. [29, 4, 3]. In a more general setting, Matthes [42] has derived existence results for networks coupled with general parabolic PDEs. Furthermore several index results exist, e.g. [4, 11].

In this chapter we will first address the index analysis of coupled network systems in Section 4.1. Moreover, we state existence results for PDAEs in refined electrical network: coupling with a) semiconductors (Section 4.2), b) telegrapher's equations (Section 4.3) and c) heat conduction (Section 4.5). Furthermore we discuss the field/circuit coupling with MQS devices in Section 4.4.

4.1 Index of electric networks coupled to electric networks

For analytic and computational purposes, one needs to check the index for the overall system as well as all subsystems. This is specially important for a dynamic iteration scheme. Since we deal with dynamic iteration of index-1 systems, we distinguish between the following conditions:

(C1) The overall system (10) has index-1.
(C2) Each subsystem (10a) is index-1 systems with respect to x_i and for u given as input. (Notice that $x_1, \ldots, x_{i-1}, x_{i+1}, \ldots, x_r$ do not enter the i-th subsystem.)
(C3) For any $i = 1, \ldots, r$, the overall system (10) is index-1 with respect to (x_i, u) where all $x_1, \ldots, x_{i-1}, x_{i+1}, \ldots, x_r$ given as input.

Notice that (C1) and (C2) do not generally imply (C3).

In the following we investigate system (9), and use system (10) only as compact notation. In the case of positive-definite generalized capacitance, inductance and conductance matrices

$$C_i(w_i,t) := \frac{\partial q_i(w_i,t)}{\partial w_i},\ L_i(w_i,t) := \frac{\partial \phi_i(w_i,t)}{\partial w_i} \text{ and } G_i(w_i,t) := \frac{\partial g_i(w_i,t)}{\partial w_i},$$

the index of the submodels $\mathcal{F}_i = 0$ depends only on the topology of the networks, and is limited by two [53, 31]. Condition (C2), i.e., $\mathcal{F}_i$ has index-1 for u given as input, holds for the i-th subcircuit, if and only if there are neither

- cut sets of flux sources and/or current and virtual voltage sources ($L_i(I_iU_i)$-cut sets), nor

- loops of only charge sources (capacitors) and at least one voltage sources (no V_iC_i-loops);

This can be reformulated in terms of incidence matrices, which reads: the matrices

$$(A_{C_i}, A_{G_i}, A_{V_i})^\top, \quad Q_{C_i}^\top A_{V_i}$$

with Q_{C_i} being a projector onto the kernel of A_{C_i} must have full column rank for $i = 1, \ldots, r$. This result can be generalized to a rather large class of controlled sources [53]

$$\imath(e_i, \jmath_{L_i}, \jmath_{V_i}, t) \quad \text{and} \quad v(e_i, \jmath_{L_i}, \jmath_{V_i}, t) \ .$$

These purely topological conditions can be easily verified for all subsystems by inspecting the partial incidence matrices.

Furthermore, the same topological conditions hold in the case of (C1), this time just globally. That is: (C1) is equivalent to the full column rank of the following two matrices:

$$\left(\begin{pmatrix} A_{C_1} & & \\ & \ddots & \\ & & A_{C_r} \end{pmatrix}, \begin{pmatrix} A_{G_1} & & \\ & \ddots & \\ & & A_{G_r} \end{pmatrix}, \begin{pmatrix} A_{V_1} & & A_{u_1} \\ & \ddots & \vdots \\ & A_{V_r} & A_{u_r} \end{pmatrix} \right)^\top \tag{30}$$

and

$$\begin{pmatrix} Q_{C_1}^\top & & \\ & \ddots & \\ & & Q_{C_r}^\top \end{pmatrix} \cdot \begin{pmatrix} A_{V_1} & & A_{u_1} \\ & \ddots & \vdots \\ & A_{V_r} & A_{u_r} \end{pmatrix}. \tag{31}$$

If condition (C2) holds, then the full rank of the matrix (30) is automatically fulfilled; the full rank of the matrix (31), however, demands that there are also no CV-loops with at least one virtual voltage source (in the overall network). This can be formulated in terms of incidence matrices and projectors. To this end, let $Q_{V_i-C_i}$, be a projector onto the kernel of $A_{V_i}^T Q_{C_i}$. We have:

Lemma 4.1. *Given that condition* (C2) *holds.*

a) Condition (C1) *is equivalent to the full column rank of* $\begin{pmatrix} Q_{V_1-C_1}^\top Q_{C1}^\top A_{u_1} \\ \vdots \\ Q_{V_r-C_r}^\top Q_{C_r}^\top A_{u_r} \end{pmatrix}$.

b) Condition (C3) *(for ith subsystem) is equivalent to the full column rank of* $Q_{V_i-C_i}^\top Q_{C_i}^\top A_{u_i}$.

Proof. The ith row of (31) is left-multiplied with projector $Q_{V_i-C_i}^T$. This gives the result. □

Remark 4.2. Note that (C3) to hold for any arbitrary subsystem is a sufficient condition for (C1), but not a necessary one.

Remark 4.3. The transformation of the coupled network equations (10) into the semi-explicit form (11) (Lemma 3.1) does not affect the index, i.e., if (10) fulfills (C1), (C2) or (C3), so does (11).

4.2 Electric networks coupled to distributed semiconductor devices

We discuss two perspectives of the coupled system of diodes (as semiconductor devices) and electric networks.

Direct view. We consider the coupled system in Box 3.1. The property

$$\boldsymbol{Q}_C^\top \boldsymbol{A}_D = 0 \tag{32}$$

ensures that the diode's current I_D (16b) contributes only to the differential part of Kirchhoff's current law (7a). This can be enforced, for example, by connecting the diode's terminals by a path of capacitors. If this topological condition (32) holds and the device current I_D is considered as given, the index-1 conditions are the usual ones [53]:

$$\ker(\boldsymbol{A}_C, \boldsymbol{A}_R, \boldsymbol{A}_V)^\top = \{0\}, \tag{33}$$

$$\ker \boldsymbol{Q}_C^\top \boldsymbol{A}_V = \{0\}. \tag{34}$$

With other words: there is no cutset of inductors and current sources, and there is no loop of capacitors containing at least one voltage source, respectively.

Specialized view. In Box 3.2, the current $\langle J \rangle (.)$ is the diode's static response. It enters the DAE network equations as source term. The dynamic part takes into account the temporal changes of the applied voltages and is related to the charge term $(\varepsilon/l)\boldsymbol{A}_D^\top \boldsymbol{u}$. Hence, for a given function $\langle J \rangle$ of the static current, structurally the semiconductor device (diode) plays the same role as a capacitance. Therefore the index-1 conditions read

$$\ker(\boldsymbol{A}_D, \boldsymbol{A}_C, \boldsymbol{A}_R, \boldsymbol{A}_V)^\top = \{0\}, \tag{35}$$

$$\ker \boldsymbol{Q}_{CD}^\top \boldsymbol{A}_V = \{0\}, \tag{36}$$

where $\boldsymbol{Q}_{CD}$ denotes a projector onto $\ker(\boldsymbol{A}_C, \boldsymbol{A}_D)^\top$. In other words, cutsets formed by independent current sources and inductors are forbidden, as well as it is forbidden to have any loops composed of capacitances, diodes and at least one voltage source. In this respect, diodes play the role of capacitances.

Existence result. To prove existence of solution for such a coupled system, one needs to control the total energy. In [3], this is only possible if the diode contributes to the differential part of the current balance, this results in the following theorem:

Theorem 4.4 (Global existence & uniqueness). *Let the source functions $\boldsymbol{\imath}$, $\boldsymbol{v}$ be continuous, the network matrices be symmetric, positive definite with conditions* (33)-(34)*, and assume constant diffusivities and mobilities. Then problem 17 admits a unique solution on the time interval* $[0, T]$ *for any* $T \in (0, \infty)$.

The proof is given in [3]: after appropriate a priori estimates and decoupling by a dedicated freezing of certain coupling variables, Banach's fixed-point theorem is employed to prove convergence of the iteration.

4.3 Electric networks coupled to telegrapher's equations

We revisit the hyperbolic transmission line network model given in Box 3.3 (Section 3.3). In addition to the coupling condition (24c) for $\boldsymbol{V}$, also the initial values have to be compatible with the boundary data, i.e.,

$$\boldsymbol{A}_\lambda^\top \boldsymbol{u}_0 = \begin{pmatrix} \boldsymbol{V}^0(0,0) \\ \boldsymbol{V}^0(l,0) \end{pmatrix}. \tag{37}$$

Naturally for a hyperbolic problem, we seek weak solutions of (24a). To be able to assign boundary conditions for the line voltage and currents, we need to have a trace in 1D. Hence we look for solutions $\boldsymbol{V}(\cdot,t), \boldsymbol{I}(\cdot,t) \in \mathcal{H} := H^1(0,l)^d$ for all $t \in [0,T]$. Now introducing test functions $\boldsymbol{w} = \begin{pmatrix} \boldsymbol{w}_1 \\ \boldsymbol{w}_2 \end{pmatrix} \in \mathcal{H} \times \mathcal{H}$ ($\boldsymbol{w}_1$ for voltages and $\boldsymbol{w}_2$ for currents) and use integration by parts, we obtain from (24a)

$$\begin{aligned} 0 = &\left\langle \begin{pmatrix} \boldsymbol{C}\boldsymbol{V}_t(\cdot,t) \\ \boldsymbol{L}\boldsymbol{I}_t(\cdot,t) \end{pmatrix}, \boldsymbol{w} \right\rangle - \left\langle \begin{pmatrix} \boldsymbol{I}(\cdot,t) \\ \boldsymbol{V}(\cdot,t) \end{pmatrix}, \boldsymbol{w}_z \right\rangle + \left\langle \begin{pmatrix} 0 \\ \boldsymbol{R}\boldsymbol{I}(\cdot,t) \end{pmatrix}, \boldsymbol{w} \right\rangle \\ &+ \left(\boldsymbol{I}(0,t)^\top,\, \boldsymbol{I}(l,t)^\top\right) \begin{pmatrix} -\boldsymbol{w}_1(0) \\ \boldsymbol{w}_1(l) \end{pmatrix} + (\boldsymbol{A}_\lambda^\top \boldsymbol{u}(t))^\top \begin{pmatrix} -\boldsymbol{w}_2(0) \\ \boldsymbol{w}_2(l) \end{pmatrix} \end{aligned} \tag{38}$$

for all $\boldsymbol{w} = \begin{pmatrix} \boldsymbol{w}_1 \\ \boldsymbol{w}_2 \end{pmatrix}$ and employing the L^2 inner product $\langle \cdot, \cdot \rangle$.

A first step towards existence results is the derivation of a-priori estimates. For linear networks with symmetric capacitance, inductance and conductance matrices $\widetilde{\boldsymbol{C}}$, $\widetilde{\boldsymbol{L}}$ and $\widetilde{\boldsymbol{G}}$, equation (38) yields for the choice $\boldsymbol{w} := (\boldsymbol{V}, \boldsymbol{I})^\top$

$$\begin{aligned} 0 = &\frac{1}{2}\frac{d}{dt}\Big\{ \langle \boldsymbol{C}\boldsymbol{V}(\cdot,t), \boldsymbol{V}(\cdot,t)\rangle + \langle \boldsymbol{L}\boldsymbol{I}(\cdot,t), \boldsymbol{I}(\cdot,t)\rangle + \boldsymbol{u}^\top \boldsymbol{A}_C \widetilde{\boldsymbol{C}} \boldsymbol{A}_C^\top \boldsymbol{u} + \boldsymbol{\jmath}_L^\top \widetilde{\boldsymbol{L}} \boldsymbol{\jmath}_L \Big\} \\ &+ \langle \boldsymbol{R}\boldsymbol{I}(\cdot,t), \boldsymbol{I}(\cdot,t)\rangle + \boldsymbol{u}^\top \boldsymbol{A}_R \widetilde{\boldsymbol{G}} \boldsymbol{A}_R^\top \boldsymbol{u} + \boldsymbol{u}^\top \boldsymbol{A}_I \boldsymbol{\imath}(t) + \boldsymbol{v}^\top(t) \boldsymbol{\jmath}_V \,. \end{aligned}$$

The symmetry of the parameter matrices implies that the differential quantities $(\boldsymbol{V}, \boldsymbol{I}, \boldsymbol{y})^\top$, $\boldsymbol{y} := (\boldsymbol{P}_C \boldsymbol{u}, \boldsymbol{\jmath}_L)^\top$ then fulfill the energy estimate

$$\rho(t) \le c \left(\rho(0) + \int_0^t \left(\rho(\tau) + \|\boldsymbol{z}(\tau)\|_2^2 \right) \, d\tau + \|\boldsymbol{\imath}\|_{L^2(0,t)}^2 + \|\boldsymbol{v}\|_{L^2(0,t)}^2 \right) \tag{39}$$

with the algebraic components given by $\boldsymbol{z} := (\boldsymbol{Q}_C \boldsymbol{u}, \boldsymbol{\jmath}_V)^\top$ and

$$\rho(t) := \|\boldsymbol{V}(\cdot,t)\|_{\mathcal{V}}^2 + \|\boldsymbol{I}(\cdot,t)\|_{\mathcal{V}}^2 + \|\boldsymbol{y}(t)\|_2^2, \quad ||\boldsymbol{f}||_{L^2(0,t)}^2 := \int_0^t \|\boldsymbol{f}(\tau)\|_2^2 \, \mathrm{d}\tau$$

with $\mathcal{V} := (L^2(0,l))^d$. To further estimate the algebraic network variables we assume the index-1 conditions (see Thm. 2.2). They guarantee the global solvability of $\boldsymbol{z}$ as a function of $\boldsymbol{y}$, $\boldsymbol{\imath}, \boldsymbol{v}$ and λ. Analogously as for the diodes case (cf. (32)), if we assume in addition

$$\boldsymbol{Q}_C^\top \boldsymbol{A}_\lambda = 0, \tag{40}$$

the dependence of $\boldsymbol{z}$ on λ is eliminated. The assumption (40) can be guaranteed by adding linear (parasitic) capacitances at all coupling nodes to transmission lines system (and possibly some parasitic resistances, such that no CV-loop is created).

Using this ($\boldsymbol{z}$ depends only on $\boldsymbol{y}(t)$, $\boldsymbol{\imath}(t)$, $\boldsymbol{v}(t)$) in (39), and applying Gronwall's lemma, the a-priori energy estimate reads:

$$\rho(t) \leq c \left(\rho(0) + \|\boldsymbol{\imath}\|^2_{L^2(0,t)} + \|\boldsymbol{v}\|^2_{L^2(0,t)} \right), \tag{41}$$

and for the algebraic variables satisfy

$$\|\boldsymbol{z}(t)\|_2^2 \leq c \left(\rho(t) + \|\boldsymbol{\imath}(t)\|_2^2 + \|\boldsymbol{v}(t)\|_2^2 \right). \tag{42}$$

Thus the coupled problem Box 3.3 is well-posed and we have [29]

Theorem 4.5. *Let the index-1 conditions (Thm. 2.2) and coupling condition* (40) *hold. Then the coupled network/transmission line problem (Box 3.3) has a unique solution* $(\boldsymbol{V}, \boldsymbol{I}, \boldsymbol{u}, \boldsymbol{\jmath}_L, \boldsymbol{\jmath}_V)^\top$*. Furthermore if the initial values and input signals fulfill*

$$\boldsymbol{V}^0, \boldsymbol{I}^0 \in \mathcal{H}, \quad \boldsymbol{\imath} \in H^1(0,T)^{n_\imath}, \quad \boldsymbol{v} \in H^1(0,T)^{n_v}$$

then $(\boldsymbol{V}, \boldsymbol{I})^\top$ *and* $(\boldsymbol{V}_t, \boldsymbol{I}_t)^\top$ *are bounded on finite time intervals with*

$$\boldsymbol{V}, \boldsymbol{I} \in \mathcal{H}, \quad \boldsymbol{V}_t, \boldsymbol{I}_t \in \mathcal{V}.$$

For the network variables it holds

$$\boldsymbol{u} \in H^1(0,T)^{n_u}\,,\ \boldsymbol{\jmath}_L \in H^1(0,T)^{n_{\jmath_L}}\,,\ \boldsymbol{\jmath}_V \in H^1(0,T)^{n_{\jmath_V}}\,.$$

Remark 4.6. 1. The energy estimates and existence and uniqueness can be transferred to the case of nonlinear networks if the charge storing elements have a symmetric capacitance matrix.
2. Motivated by the a priori estimates, an PDAE-perturbation index can be introduced, for details see [32].

4.4 Electric Networks Coupled to Magnetic Fields (MQS)

We return to the MQS device introduced in Section 3.4 (Box 3.4). First we note that the curl-curl equation (26) with Coulomb gauge, boundary and initial condition was shown to be well-posed, [15]. Thus the system is also qualified for circuit coupling. Main results for this coupled problem are known for the semi-discrete case. Thus in the following we introduce the spatially discretized version and summarize some known results.

Semi-discretized MQS Device Model

A spatial discretization is performed by employing the finite integration technique [54]. This method uses staggered grids to define discrete quantities in Maxwell's equations (1) via integration. Accord-

ing to the role of the quantity, integration is performed along certain edges and faces. This yields the so-called Maxwell grid equations, which show a one-to-one correspondence to its continuous version (for details see [54, 55]). Thus also the curl-curl equation (26) has a representation as:

$$\mathbf{M}_\sigma \frac{d}{dt}\widehat{\mathbf{a}} + \mathbf{K}(\widehat{\mathbf{a}})\widehat{\mathbf{a}} = -\mathbf{M}_\sigma \mathbf{G}\mathbf{\Phi} \quad \text{with} \quad \mathbf{K}(\widehat{\mathbf{a}}) = \tilde{\mathbf{C}}(\mathbf{M}_\nu)\mathbf{C}.$$

This employs discretizations of the curl operator on the primal grid $\mathbf{C}$ and on the dual grid $\tilde{\mathbf{C}}$, the gradient operator $\mathbf{G}$ (primal grid), the line integral of the magnetic vector potential $\mathbf{A}$ for a primal edge e, and discrete scalar potential (primal node):

$$\widehat{\mathbf{a}}_e := \int_e \mathbf{A} \cdot \mathrm{d}\mathbf{s}, \qquad \mathbf{\Phi}_{\mathrm{n_i}} = \phi(\mathbf{r}_{n_i}).$$

Furthermore a suitable material approximation $\mathbf{M}_\sigma$ for the conductivity σ is used, e.g. [22]. In the coupling with the electric network in (27a) (Box 3.4), the right-hand side term reads $\sigma\chi_{\mathrm{M}}v_{\mathrm{m}}$. Thus we need also a discrete version of χ_{M}. Let the primal grid consist of n_e edges, any path $\bar{\gamma}$ in this grid can be described as an element in $\{-1, 0, 1\}^{n_e}$ (where -1 indicates that an edge is traversed in the opposite direction. For a path $\bar{\gamma}$, which lies inside Ω_M and which connects both contacts, we can define $\mathbf{X}$ as line integrals for any primal edge e_i

$$\mathbf{X}_i = \bar{\gamma}_i \int_{e_i} \chi_{\mathrm{M}} \mathrm{d}s,$$

which gives a discretization of χ_{M}. Notice $\sum_i \mathbf{X}_i = 1$, since χ_{M} was derived from applying one volt. Further possibilities for $\mathbf{X}$ one finds in [50, 12]. Then the coupling term reads $\mathbf{M}\mathbf{X}A_{\mathrm{M}}^\top u$. This excitation is inserted into the curl-curl equation and gives (43a) in Box 4.1. On the other hand, the coupling current in ($27\mathrm{b}_2$) becomes the term $i_{\mathrm{M}} = \mathbf{X}^\top \mathbf{K}(\widehat{\mathbf{a}})\widehat{\mathbf{a}}$. Finally the MQS-device current enters the current balance of the network equations (see Box 4.1). A structural analysis of this system is given in [12].

Box 4.1: Semi-discretized MQS-Coupling.

Semi-discrete MQS-Model:

$$\mathbf{M}\frac{d}{dt}\widehat{\mathbf{a}} + \mathbf{K}(\widehat{\mathbf{a}})\widehat{\mathbf{a}} - \mathbf{M}\mathbf{X}A_{\mathrm{M}}^\top u = 0, \tag{43a}$$

Coupling:

$$v_{\mathrm{M}} = A_{\mathrm{M}}^\top u, \qquad i_{\mathrm{M}} = \mathbf{X}^\top \mathbf{K}(\widehat{\mathbf{a}})\widehat{\mathbf{a}} \tag{43b}$$

DAE-IVP problem for the network: given by DAE (7) plus updating:

$$A_I \rightsquigarrow (A_I \quad A_M), \qquad \imath(t) \rightsquigarrow \begin{pmatrix} \imath(t) \\ i_M(t) \end{pmatrix} \tag{43c}$$

Remark 4.7. a) Via the structure of the conductivity matrix $\mathbf{M}$, one can obtain either stranded or foil conductor models. However, by algebraic transformations, one can always achieve the above coupling structure in Box 4.1, [50].

b) The discrete sparse coupling [21] imposes the voltages only onto the edges crossing a reference plane, see also [12].

c) For the coupling, we demand that our paths $\bar{\gamma}$ do not leave Ω_M, i.e., for an projector Q_M onto $\ker(\mathbf{M})$

$$\mathbf{X} = \mathbf{X}P_M \qquad P_M := I - Q_M. \tag{44}$$

This is referred to as soundness of the excitation, [12].

MQS-Network Index Analysis

We report a result on the tractability index from [12]:

Theorem 4.8. *Let Assumption 2.1 hold, a gauging be given, and let the excitation be sound* (44)*. The index of the DAE* (43) *is quantified as follows:*

a) It is index-0 if and only if there is a spanning tree of capacitors, and no MQS device and no voltage source.

b) Furthermore let the network contain either a MQS device or a voltage source or let the network contain no spanning tree of capacitors. The respective index is 1 if and only if there is neither a cutset of inductors, current sources and MQS devices (LIM-cutset) nor a CV-loop.

c) Let the network contain at least one MQS device, one voltage source or no spanning tree of capacitors only. The respective system has index-2 if and only if there is an LIM-cutset or a CV-loop.

4.5 Electric Networks Coupled to Heat Transport

Here we address the well posedness of the thermal element as stand alone and the coupled problem.

Well-posedness of the thermal element

We consider the linear heat equation (29a) for Box 3.5 with with constant thermal diffusivity λ, heat exchange with the environment cT and for $x \in \Omega$. The problem is equipped by initial and boundary conditions:

$$T(\mathbf{x}, 0) = T_0(\mathbf{x}), \quad \text{in } \Omega, \qquad T + \alpha \frac{\partial T}{\partial n} = g(t), \quad \text{on } \partial\Omega \times (0, t_e), \tag{45}$$

with ambient temperature g and average temperature θ_k as introduced in (28) and $\alpha > 0$.

To check the well-posedness of the thermal element, it was only driven by independent sources and checked that in any case solutions to the driven problem exist [19]. By driven, it is meant that the following two settings for the heat equation are considered:

1) given p, compute T and θ from (29a) with IC and BC (45)
2) given θ, compute T and p from (29a) with IC and BC (45).

We summarize the results of that work in the following. To this end, assumptions are needed: Let Ω be closed and Lipschitz, and let the device areas be closed sets $\Omega_k \subseteq \Omega$ with nonempty interior and piecewise disjoint.

In practice, the instantaneous power terms $p_k(t)$ are computed from the network variables, which depend in turn on the device temperatures θ_k. For the well-posedness, this perspective is simplified by assuming the following constitutive relation to close the system:

$$a_k p_k(t) + \ b_k \theta_k(t) = s_k(t) \qquad (k = 1, \ldots, n) \tag{46}$$

with given constant coefficients a_k, b_k and given functions s_k, which represent the above mentioned independent source terms. Moreover, it is assumed that not both coefficients a_k and b_k vanish at the same time. Obviously, $a_k = 0$ results in assigning a fixed average temperature to Ω_k (in the terminology of electric networks, it represents a voltage source). Assigning $b_k = 0$ yields a fixed Joule power dissipated (which is equivalent to a current source).

Following [19], a uniqueness result is stated for an elliptic setting with instantaneous heat changes in the weak form. Then we have

Theorem 4.9. *Given functions s_k $(k = 1, \ldots, n)$ and g. Then there exist a unique $T \in \mathbb{H}^1(\Omega)$ and unique $p_k \in \mathbb{R}$, $k = 1, \ldots, n$, such that in corresponding weak form holds:*

$$\begin{aligned} -\lambda \Delta T + \gamma T &= f + \textstyle\sum_{k=1}^{n} p_k \, \mathbf{1}_{\Omega_k}, && \text{in } \Omega, \\ T + \alpha \frac{\partial T}{\partial n} &= g, && \text{on } \partial\Omega, \\ \int_{\Omega_k} T \, d\Omega = \theta_k, \quad a_k p_k + b_k \theta_k &= s_k, \quad k = 1, \ldots, n, \end{aligned} \tag{47}$$

with $\gamma \in \mathbb{L}^\infty(\Omega)$, $f \in \mathbb{L}^2(\Omega)$, $\alpha \geq 0$ and $g \in \begin{cases} \mathbb{L}^2(\partial\Omega), & \alpha > 0, \\ \mathbb{H}^{1/2}(\partial\Omega), & \alpha = 0. \end{cases}$

Remark 4.10 (Proof of Thm 4.9). The proof in [19] first considers the case, where the constitutive relation (with s_k) is replaced by a given θ_k. Then the linearity of the differential operator is used to split (47) in a number of n standard-problems. In each a Dirac-type problems is solved, where just the kth power term is applied at a level of one. These problem can be solved by standard arguments. Then the sought solution is a linear combination of standard-problem solutions. Now to obtain the values p_k, a linear system needs to be solved. By construction, it can be show that the system matrix is regular. Finally, this is transferred to the original constitutive relation. For details we refer to [19, 20].

This analysis qualifies the above model as a choice for circuit simulation. Furthermore, to seamlessly fit the thermal element into the circuit simulation flow, a thermal element stamp can be designed, see [20].

Coupled Problem Analysis

For an index-1 network with averaging for the thermal coupling (and several other assumptions), one can show that the coupled problem admits a solution. This was show for a slightly more abstract thermal model in [10] based on 1D structures only. For a general thermal element in 2D or 3D as discussed here, existence is found in [20]. In both works the standard proof for a parabolic setting is extended to the DAE case (index-1). To this end, the network variables are parsed and coupling assumptions are needed. Furthermore this was generalized in the work of Matthes [42].

4.6 Further Reading

We address a couple of aspects. The existence result for semiconductor models in electric networks can be generalized to more advanced semiconductor models in multiple dimensions, e.g. [5] and with multiple contacts, e.g. [1]. Furthermore, also an existence result for index-2 networks coupled with semiconductor devices is known [6]. There the coupling should not be affected from the index two variables.

There are many papers on index definitions for PDAEs. We refer to an index analysis in [17].

5 Cosimulation

In the multiphysical framework of refined electrical network modelling discussed in chapter 3, one is confronted with PDAE systems, which are transferred into coupled DAE systems by a method-of-lines approach. Dynamic iteration schemes are one idea to efficiently approximate these coupled systems in an iterative way. Furthermore this technique allows to reuse dedicated, preferred simulation code and thus enables multimethod, multirate and so on. This technique is also referred to as cosimulation. Here we summarize most important results for coupled DAE systems, which occur in refined network analysis.

5.1 Description of coupled DAE systems for dynamic iteration schemes

We assume the semi-explicit formulation for the network part discussed in Lemma 3.1. Thus after a (vertical) method-of-lines, we are finally confronted with a set of $r = 2$ coupled DAE subsystems: one describing the network, and the other describing distributive effects (semiconductor devices, transmission lines, heat transport, magnetoquasistatic fields). This reads:

$$\begin{aligned} \dot{\mathbf{y}}_1 &= \mathbf{f}_1(\mathbf{y}, \mathbf{z}), & \dot{\mathbf{y}}_2 &= \mathbf{f}_2(\mathbf{y}, \mathbf{z}), \\ 0 &= \mathbf{g}_1(\mathbf{y}, \mathbf{z}), & 0 &= \mathbf{g}_2(\mathbf{y}, \mathbf{z}). \end{aligned} \tag{48}$$

To get an overall index-1 system, we assume the functions $\mathbf{f} := (\mathbf{f}_1, \mathbf{f}_2)^\top$ and $\mathbf{g} := (\mathbf{g}_1, \mathbf{g}_2)^\top$ to be sufficiently often differentiable and the Jacobian $\partial\mathbf{g}/\partial\mathbf{z}$ (with $\mathbf{y} := (\mathbf{y}_1, \mathbf{y}_2)^\top$, $\mathbf{z} := (\mathbf{z}_1, \mathbf{z}_2)^\top$) to be non-singular in the neighborhood of the solution. In order to ensure index-1 for each subsystem in addition, it has to hold

$$\partial\mathbf{g}_1/\partial\mathbf{z}_1 \text{ and } \partial\mathbf{g}_2/\partial\mathbf{z}_2 \text{ are non-singular,} \tag{49}$$

i.e., $\mathbf{g}_1(\mathbf{y}, \mathbf{z}) = 0$ is locally, uniquely solvable for $\mathbf{z}_1$ (for given $\mathbf{y}$, $\mathbf{z}_2$) and $\mathbf{g}_2(\mathbf{y}, \mathbf{z}) = 0$ for $\mathbf{z}_2$ (for given $\mathbf{y}$, $\mathbf{z}_1$).

Remark 5.1 (Overlapping). In some settings, certain quantities (and corresponding algebraic constraints) can be assigned to several subsystems. This is called overlapping. It introduces additional degrees of freedom to the latter dynamic iteration scheme, see e.g. [9]. Here, these aspects are not discussed.

5.2 Definition of dynamic iteration schemes

In dynamic iteration schemes, the iteration is based on the splitting of the whole integration interval $[t_0, t_e]$ into so-called time windows

$$[t_n, t_{n+1}] \qquad \text{with} \qquad t_0 < t_1 < t_2 < \ldots < t_N = t_e$$

and with related window sizes $H_n := t_{n+1} - t_n$. Assuming the numerical approximation is already computed on $[0, t_n]$, a dynamic iteration defines on the next window $(t_n, t_{n+1}]$ the approximations $(\tilde{\mathbf{y}}, \tilde{\mathbf{z}})|_{(t_n, t_{n+1}]}$ via an extrapolation and subsequent iterations. In detail, we have the steps:

- *extrapolation step*: the initial guess for the dynamic iteration on $(t_n, t_{n+1}]$ is defined by an extrapolation Φ_n from $[t_{n-1}, t_n]$ to $(t_n, t_{n+1}]$,

$$\begin{pmatrix} \tilde{\mathbf{y}}_n^{(0)} \\ \tilde{\mathbf{z}}_n^{(0)} \end{pmatrix} := \Phi_n \begin{pmatrix} \tilde{\mathbf{y}}|_{(t_{n-1}, t_n]} \\ \tilde{\mathbf{z}}|_{(t_{n-1}, t_n]} \end{pmatrix}. \tag{50}$$

  The extrapolation operator Φ_n is assumed to be continuous, to be uniform Lipschitz with constant L_Φ and to be accurate of at least order $\mathcal{O}(H_n^1)$.
- *iteration step*: for a finite iteration number k_n, the map Ψ_n defines the transition from old iterates $(k-1)$ to new iterates (k):

$$\begin{pmatrix} \tilde{\mathbf{y}}_n^{(k-1)} \\ \tilde{\mathbf{z}}_n^{(k-1)} \end{pmatrix} \to \begin{pmatrix} \tilde{\mathbf{y}}_n^{(k)} \\ \tilde{\mathbf{z}}_n^{(k)} \end{pmatrix} \qquad \text{with} \qquad k = 1, \ldots, k_n \tag{51}$$

  via the solution of our coupled IVPs (48). To this end, we have to introduce splitting vectors $(\tilde{\mathbf{Y}}_{1,n}^{(k)}, \tilde{\mathbf{Z}}_{1,n}^{(k)})$ and $(\tilde{\mathbf{Y}}_{2,n}^{(k)}, \tilde{\mathbf{Z}}_{2,n}^{(k)})$, which allow us to address old and new iterates and result in the split formulation:

$$\dot{\tilde{\mathbf{y}}}_{1,n}^{(k)} = \mathbf{f}_1(\tilde{\mathbf{Y}}_{1,n}^{(k)}, \tilde{\mathbf{Z}}_{1,n}^{(k)}), \quad \text{with} \quad \tilde{\mathbf{y}}_{1,n}^{(k)}(t_n) = \tilde{\mathbf{y}}_{1,n}^{(k-1)}(t_n), \tag{52a}$$

$$0 = \mathbf{g}_1(\tilde{\mathbf{Y}}_{1,n}^{(k)}, \tilde{\mathbf{Z}}_{1,n}^{(k)}), \tag{52b}$$

$$\dot{\tilde{\mathbf{y}}}_{2,n}^{(k)} = \mathbf{f}_2(\tilde{\mathbf{Y}}_{2,n}^{(k)}, \tilde{\mathbf{Z}}_{2,n}^{(k)}), \quad \text{with} \quad \tilde{\mathbf{y}}_{2,n}^{(k)}(t_n) = \tilde{\mathbf{y}}_{2,n}^{(k-1)}(t_n), \tag{52c}$$

$$0 = \mathbf{g}_2(\tilde{\mathbf{Y}}_{2,n}^{(k)}, \tilde{\mathbf{Z}}_{2,n}^{(k)}). \tag{52d}$$

The choice of the splitting vectors defines the type of the dynamic iteration scheme applied, e.g. for a Gauss-Seidel type we have

$$\begin{aligned} \tilde{\mathbf{Y}}_{1,n}^{(k)} &= (\tilde{\mathbf{y}}_{1,n}^{(k)}, \mathbf{y}_{2,n}^{(k-1)})^\top, & \tilde{\mathbf{Z}}_{1,n}^{(k)} &= (\tilde{\mathbf{z}}_{1,n}^{(k)}, \mathbf{z}_{2,n}^{(k-1)})^\top, \\ \tilde{\mathbf{Y}}_{2,n}^{(k)} &= (\tilde{\mathbf{y}}_{1,n}^{(k)}, \mathbf{y}_{2,n}^{(k)})^\top, & \tilde{\mathbf{Z}}_{2,n}^{(k)} &= (\tilde{\mathbf{z}}_{1,n}^{(k)}, \mathbf{z}_{2,n}^{(k)})^\top. \end{aligned} \tag{53}$$

Finally, the numerical approximation on the window $[t_n, t_{n+1}]$ reads:

$$\begin{pmatrix} \tilde{\mathbf{y}}|_{(t_n,t_{n+1}]} \\ \tilde{\mathbf{z}}|_{(t_n,t_{n+1}]} \end{pmatrix} := \begin{pmatrix} \tilde{\mathbf{y}}_n^{(k_n)} \\ \tilde{\mathbf{z}}_n^{(k_n)} \end{pmatrix}.$$

5.3 Stability and convergence analysis

For coupled ODEs, the dynamic iteration methods discussed above is convergent on a bounded time interval provided Lipschitz continuity is given [40]. By choosing appropriate window sizes, the convergence can be enhanced. However, for DAEs an additional contractivity must be satisfied to obtain (a) the convergence of iterations within a window and (b) to guarantee the stable error propagation in algebraic variables (window to window), see e.g. [8, 37, 39]. If we neglect errors from time integration, i.e., we iterate on analytic waveforms, one obtains a related error recursion with the following main result (for further details see [12], or [8] for a Lagrangian type of coupling):

Theorem 5.2 (Stability and convergence).

a) Stable error recursion within one time window $(t_n, t_{n+1}]$: Given α, if the following contractivity condition holds (for any k)

$$\alpha_{n,k} := \left\| \left(\frac{\partial \mathbf{g}}{\partial \mathbf{z}} \cdot \frac{\partial \tilde{\mathbf{Z}}_n}{\partial \tilde{\mathbf{z}}_n^{(k)}} \right)^{-1} \cdot \left(\frac{\partial \mathbf{g}}{\partial \mathbf{z}} \cdot \frac{\partial \tilde{\mathbf{Z}}_n}{\partial \tilde{\mathbf{z}}_n^{(k-1)}} \right) \right\| < \alpha < 1, \tag{54}$$

the error within one time window converges to zero as the number of iterations k approaches infinity. For $\alpha_{n,k} \neq 0$, the rate of convergence is then given by $\alpha_{n,k} + \mathcal{O}(H)$. For $\alpha_{n,k} = 0$, one obtains $\mathcal{O}(\sqrt{H})$ as rate of convergence in the general case.

b) Convergence of dynamic iteration schemes: Supposed that the above contractivity condition holds, the dynamic iteration is convergent on the whole integration interval provided that k_n iterations are performed on the n-th time window with k_n fulfilling the inequality

$$L_\Phi \alpha_n^{k_n} \leq \alpha \qquad \left(\alpha_n := \max_{k \leq k_n} a_{n,k} \right). \tag{55}$$

Notice that the necessary number of iterations is linked to both the Lipschitz constant L_Φ (extrapolation operator) and the contractivity number α_n.

If the contractivity number $\alpha_n = 0$, a better convergence rate $\mathcal{O}(H^p)$ with $p > 1/2$ can be obtained. The actual rate depends on the fine structure of the coupled DAE systems. We report on a main result from [13]:

Theorem 5.3 (Fine structure analysis). *Given a Gauss-Seidel dynamic iteration schemes, for the rate of convergence p_r holds:*

i) $p_r = 1$ *(i.e.,* $\mathcal{O}(H)$*), if* $\dfrac{\partial \mathbf{g}_1}{\partial \mathbf{z}_2} = 0$;

ii) $p_r = 2$ *(i.e.,* $\mathcal{O}(H^2)$*), if in addition holds:*

$$(a)\ \frac{\partial \mathbf{f}_1}{\partial \mathbf{z}_2} = 0,\ \frac{\partial \mathbf{f}_2}{\partial \mathbf{z}_1} = 0,\ \frac{\partial \mathbf{g}_1}{\partial \mathbf{y}_2} = 0 \ \text{ or } \ (b)\ \frac{\partial \mathbf{g}_1}{\partial \mathbf{y}_2} = 0,\ \frac{\partial \mathbf{g}_2}{\partial \mathbf{y}_1} = 0,\ \frac{\partial \mathbf{g}_2}{\partial \mathbf{z}_1} = 0.$$

Up to now, we have neglected the influence of the approximation error introduced by using numerical time integration schemes instead of exact waveforms. It was shown in [51] that an optimal choice of the convergence order of time integration methods in dynamic iteration schemes has to be based both on the iteration number k and the rate of convergence p of the dynamic iteration schemes:

Theorem 5.4. *Let a coupling structure be given, where the dynamic iteration scheme has convergence rate p_r. Then k iterations yield the order $\mathcal{O}(H^{k \cdot p_f})$. If an numerical time integration scheme of convergence order $k \cdot p_f$ is used, then the total time integration error is the same order ($\mathcal{O}(H^{k \cdot p_f})$).*

That is, the theorem states the minimal and sufficient convergence to achieve a desired rate of convergences (given the coupling structure).

6 Conclusions

In our paper we have given an overview of PDAE models in circuit simulation. We started from the derivation of mathematical descriptions of the corresponding electric system. In this context three types of coupling can be distinguished: (1) network-to-network, (2) coupling to refined models and (3) coupling to other physical domains (multiphysical models). Then we have discussed the structural and analytic properties of the introduced models. Last, we discussed the application of the cosimulation technique, which is dedicated to coupled systems and enables the coupling of dedicated solvers. However, its draw back are contractivity conditions, which need to be fulfilled in the context of DAEs to guarantee convergence. A fine structure analysis reveals the convergence rates, which is important for an adaptive selection of communication step sizes within the cosimulation.

Finally we note that in the context of the network approach very naturally the coupled systems are a combination of DAE and PDE. Furthermore similar PDAE systems occur in many other applications and technologies.

Acknowledgements We thank Giuseppe Alì (Università della Calabria, Italy) and Sebastian Schöps (TU Darmstadt) for many fruitful discussions over the past years. Furthermore, we like to acknowledge the support

of the German Federal Government within the mathematics programme, project grants 03MS648E (SOFA), 05M13PXA (KoSMOS) and 05M13PXB (SIMUROM).

References

1. Alì, G.: PDAE models of integrated circuits. J. Math. Comp. Model., 51:7-8 (2010), pp. 915–926.
2. Alì, G., Bartel, A., Culpo, M., Günther, M., Schöps, S.: Dynamic iteration schemes for PDAEs. To appear in: M. Günther (ed.): COMSON-Handbook, Springer, Berlin, 2014.
3. Alì, G., Bartel, A., Günther, M.: Parabolic differential-algebraic models in electric network design. SIAM J. MMS 4 (2005) 3, pp. 813–838.
4. Alì, G., Bartel, A., Günther, M., Tischendorf, C.: Elliptic partial differential-algebraic multiphysics models in electrical network design. Math. Model. Meth. Appl. Sc. 13 (2003) 9, pp. 1261–1278.
5. Alì, G., Bartel, A., Rotundo, N.: An existence result for index-2 PDAE system arising in semiconductor modeling. In: [30], pp. 46–51
6. Alì, G., Bartel, A., Rotundo, N.: Index-2 elliptic partial differential-algebraic models for circuits and devices. Preprint BU Wuppertal. Submitted to SIAP.
7. Alì, G., Rotundo, N.: An existence result for elliptic partial differential-algebraic equations arising in semiconductor modeling. Nonlinear Anal., **72** (2010), pp. 4666–4681.
8. Arnold, M., Günther, M.: Preconditioned dynamic iteration for coupled differential-algebraic systems. BIT Numerical Mathematics, **41**:1, pp. 1–25 (2001).
9. Arnold, M., Heckmann, A.: From Multibody Dynamics to Multidisciplinary Applications. In: García Orden, J.C., Goicolea, J.M., Cuadrado, J. (eds.): Multibody Dynamics. Computational Methods and Applications, Springer-Verlag, pp. 273–294 (2007).
10. Bartel, A.: Partial Differential-Algebraic Models in Chip Design - Thermal and Semiconductor Problems, PhD Thesis at TU Munich, VDI-Verlag, Düsseldorf, 2004.
11. Bartel, A., Baumanns, S., Schöps S.: Structural Analysis of Electrical Circuits Including Magnetoquasistatic Devices, Appl. Num. Math., 61, 2011, pp. 1257–1270.
12. Bartel, A., Brunk, M., Günther M., Schöps, S.: Dynamic Iteration for Coupled Problems of Electric Circuits and Distributed Devices. SIAM J. Sci. Comput., 35(2), 2013, B315-B335.
13. Bartel, A., Brunk, Schöps, S.: On the convergence rate of dynamic iteration for coupled problems with multiple subsystem. Accepted for Publication at JCAM 2013.
14. Bíró, O., Preis, K.: On the use of the magnetic vector potential in the finite-element analysis of three-dimensional eddy currents. IEEE Trans. Magn., 25:4, pp. 3145–3159 (1989).
15. Bíró, O., Valli, A.: The Coulomb gauged vector potential formulation for the eddy-current problem in general geometry: Well-posedness and numerical approximation, Comput. Meth. Appl. Mech. Eng., 13:16, pp. 1890–1904 (2007).
16. B. Simeon, C. Führer, P. Rentrop: Differential-algebraic equations in vehicle system dynamics. Surveys on Mathematics for Industry 1 (1991) 1–37.
17. Bodestedt, M., Tischendorf, C.: PDAE models of integrated circuits and index analysis. Math. Comput. Model. Dyn. Syst. 13:1, pp. 1–17 (2007).
18. Büttner, J., Simeon, B.: Numerical Treatment of Material Equations with Yield Surfaces. in: Hutter, K.; Baaser, H. (eds.); Deformations and failure of metallic continua, Lecture Notes in Appl. Comp. Mech. 10, Springer-Verlag, Berlin 2003.
19. Culpo, M., de Falco, C.: Dynamical iteration schemes for coupled simulation in nanoelectronics. PAMM 8:1 (2008), pp. 10065–10068.
20. Culpo, M.: Numerical Algorithms for System Level Electro-Thermal Simulation, PhD Thesis at BU Wuppertal (2009). `http://http://elpub.bib.uni-wuppertal.de/`
21. De Gersem, H., Weiland, T.: Field-circuit coupling for time-harmonic models discretized by the finite integration technique, IEEE Trans Magn, 40 (2004), pp. 1334–1337.
22. De Gersem, H., Munteanu, I., Weiland, T.: Construction of Differential Material Matrices for the Orthogonal Finite Integration Technique with Linear Materials. IEEE Trans Magn, 44:6 (2008), pp. 710–713.
23. Engl, G.: The modeling and numerical simulation of gas flow networks. Numer. Math. 72 (1996), pp. 349–366.

24. Estévez Schwarz, D., Tischendorf, C.. Structural analysis of electric circuits and consequences for MNA. International Journal of Circuit Theory and Applications, 28:2, pp. 131–162, 2000.
25. Fukahori, K.: Computer simulation of monolithic circuit performance in the presence of electro-thermal interactions. PhD thesis, University of California, Berkeley (1977).
26. Griepentrog, E., März, R.: Differential-Algebraic Equations and Their Numerical Treatment, Teubner, Leipzig, 1986.
27. Grabinski, H.: Theorie und Simulation von Leitbahnen. Signalverhalten von Leitungssystemen in der Mikroelektronik. Springer-Verlag, Berlin, 1991.
28. Grasser, T.; Selberherr, S.: Fully coupled electrothermal mixed-mode device simulation of SiGe HBT circuits. IEEE Trans. on Electron Devices 48 (2001), pp. 1421–1427.
29. Günther, M.: Partielle differential-algebraische Systeme in der numerischen Zeitbereichsanalyse elktrischer Schaltungen. VDI-Verlag, Düsseldorf, 2001.
30. Günther, M., Bartel, A., Brunk, M., Schöps, S., Striebel, S.: Progress in Industrial Mathematics at ECMI 2010, Springer, Berlin, 2012.
31. Günther, M., Feldmann, U.: CAD based electric circuit modeling in industry I: Mathematical structure and index of network equations. Surv. Math. Ind. 8 (1999), pp. 97–129.
32. Günther, M.; Wagner, Y.: Index concepts for linear mixed systems of differential-algebraic and hyperbolic-type equations. SIAM J. Sci. Comp. 22 (2000) 5, pp. 1610–1629.
33. Hairer, E., and Wanner, G.: Solving ordinary differential equation: II, Stiff and differential-algebraic problems, 2. rev. ed., Springer, 2002.
34. Haus, H.A., Melcher, J.R.: Electromagnetic Fields and Energy, Prentice Hall, 1989.
35. Igic, P.M., Mawby, P.A., Towers, M.S., Batcup, S.: Dynamic electro-thermal physically based compact models of the power devices for device and circuit simulations, P IEEE SEM (2001), pp. 35–42.
36. Ilchmann, A., Reis, T.: Surveys in Differential-Algebraic Equations I. DAE-F (Differential Algebraic Equations Forum), Springer, Heidelberg, 2013.
37. Jackiewicz, Z., Kwapisz, M., Convergence of waveform relaxation methods for differential-algebraic systems, SIAM J. Numer. Anal., 33 (1996), pp. 2303–2317.
38. Jansen L.; Tischendorf, C.: A unified (P)DAE modeling approach for flow networks. Talk at *Descriptor Systems Workshop 2013*, Eringerfeld, Germany.
39. Lelarasmee, E.: The Waveform Relaxation Method for Time Domain Analysis of Large Scale Integrated Circuits: Theory and Applications, Ph.D. thesis, University of California, Berkeley, 1982.
40. Lelarasmee, E., Ruehli, A., and Sangiovanni-Vincentelli, A.: The waveform relaxation method for time domain analysis of large scale integrated circuits, IEEE Trans. on CAD of IC and Syst., 1 (1982), pp. 131–145.
41. Markowich, P.A., Ringhofer, C.A., Schmeiser, C.: Semiconductor Equations, Springer, 1990.
42. Matthes, M.: Numerical Analysis of Nonlinear Partial Differential Algebraic Equations: A Coupled and an Abstract Systems Approach. PhD thesis, Logos Verlag Berlin, 2012.
43. Rentrop, P., and Steinebach, G., Model and numerical techniquesfor the alarm system of river Rhine. Surv. Math. Ind. 6, (1997), pp. 245–265.
44. Riaza, R.: DAEs in Circuit Modelling: A Survey. In [36], pp. 97–136.
45. Quarteroni, A.; Ragni, S.; Veneziani, A.: Coupling between lumped and distributed models for blood flow problems. Comput. Vis. Sci. 4 (2001). pp. 111–124.
46. Reinschke, K., Schwarz, P.: Verfahren zur Rechnergestützen Analyse linearer Netzwerke. Akademie Verlag Berlin, 1976.
47. International Technology Roadmap for Semiconductors, 2012, see `http://www.itrs.net/`
48. Roos, J., Costa, L.R. (Eds.): Scientific Computing in Electrical Engineering SCEE 2008, Springer, Berlin, 2010.
49. Selberherr, S.: Analysis and Simulation of Semiconductor Devices, Springer, 1984.
50. Schöps, S., Bartel, A., De Gersem, H., Günther, M.: DAE-index and convergence analysis of lumped electric circuits refined by 3-d MQS conductor models. In: [48], pp. 341–350.
51. Schöps, S., Bartel, A., Günther, M.: On the convergence order of time-integration in dynamic iteration schemes with the windowing technique. To appear in Proceedings in Applied Mathematics and Mechanics, volume 13, number 1, 2013.
52. Schöps, S.: Multiscale Modeling and Multirate Time-Integration of Field/Circuit Coupled Problems, VDI Verlag, Düsseldorf, 2011.

53. Tischendorf, C.: Topological index calculation of differential-algebraic equations in circuit simulation. Surv. Math. Ind., 8 (1999), pp. 187–199.
54. Weiland, T.: A discretization model for the solution of Maxwell's equations for six-component fields. AEU, 31 (1977), pp. 116 – 120.
55. Weiland, T.: Time Domain Electromagnetic Field Computation with Finite Difference Methods. In: Int. J. Numer. Model.: Electronic Netowrks, Devices and Fields, 9:4 (1996), pp. 295–319.